Predicting subject-specific brain functional connectivity from structural connectivity: A deep learning perspective

by

Md Soumik Farhan

A Thesis submitted to the Faculty of Graduate Studies of
The University of Manitoba
in partial fulfilment of the requirements of the degree of

Master of Science

Biomedical Engineering Graduate Program

Price Faculty of Engineering

University of Manitoba

Abstract

Previous neuroscientific studies have reported strong relationships between brain structure and function. In humans, this has most commonly been done using non-invasive, MRI-based measures of resting-state functional connectivity (FC) and structural connectivity (SC) in combination with computational modeling, and more recently artificial intelligence (AI) methods, to explore SC-FC correlations and attempts to predict one form of connectivity (e.g., FC) from the other (e.g., SC). However traditional computational modeling-based studies evaluated the results based on "conventional parameters" (statistical measurements such as: mean squared error, correlation, variance) which are prone towards floor effect. Due to the tremendous preprocessing steps involved in data processing pipelines, there lies a definitive need for a standard dataset for comparing connectivity-based analysis and evaluating the efficacy of the experimental methods.

To overcome these problems, a curated open dataset (containing SC, and different forms of FC), a set of traditional performance parameters along with a novel parameter are proposed. Using a practical example (structural (diffusion MRI) and functional (resting-state fMRI) connectomes from 762 participants in the Human Connectome Project (HCP, S900 release) – regions of interests parcellated from Glasser atlas), we wanted to establish the baseline performance through a Graph Convolutional Network (GCN) & U-Net. For optimizing the baseline performance and improving the performance of the algorithm, we systematically modified these two different AI-based methods (6 GCN's and 2 U-Net's; in total 8 configurations) to establish a more optimized deep learning-based approach for predicting subject-specific brain FC from SC. These eight configurations were evaluated using both conventional performance

metrics as well as the recently proposed pairwise functional connectome fingerprinting approach (PFCF) to determine how closely matched each subjects predicted and measured FCs are, relative to inter-subject differences in measured FCs. These results show that for SC-FC prediction, all of the GCN architectures worked better than the U-Nets. Although traditional performance metrics have indicated differences in performance for each structural variation, PFCF is quantitatively more rigorous. Therefore, we conclude that the current analysis based on a comprehensive set of metrics on the standardized dataset will provide a new benchmark for future AI-based connectivity prediction.

Acknowledgements

There are several people without whom this thesis might not have been written, and to whom I am greatly indebted.

First and foremost, my Supervisor Dr. Chase Figley, for whom I was able to indulge myself in such an interesting project involving neuroimaging. Secondly, my co-supervisor Dr. Ahmed Ashraf for giving me the constant direction regarding the analysis of the project with machine learning. Before starting this journey, I was skeptical about my experience on both neuroimaging and machine learning. It was an interesting project with different aspects and unique challenges, and I am greatly indebted to both for having all of the long Friday afternoon conversations. It helped me to learn different aspects of any problem and ways to solve them. I could not ask for more and would like to take this opportunity to say a humble 'Thank you' to both of you.

I would like to thank my committee members Dr. Jennifer Kornelsen & Dr. Ji Hyun Ko for their precious time reading my proposal, checking on my progress, examining my thesis, and providing feedback at all the stages.

I would like to acknowledge Dr. Petra Ritter *(Charite–Universittsmedizin Berlin)* and her team for providing the preprocessed and segmented SC edge-weight and FC time-course HCP data used in this research.

I would like to recognize NSERC *(Discovery Grant)* and the Thorlakson Foundation *(Operating Grant)* for funding our work, and the Compute Canada Research Computing Cluster for the availability of the computational resources.

I would like to acknowledge the continuous motivation and support from my acquaintances in Winnipeg and at the University of Manitoba, friends abroad (especially

Rezwana Nasrin) for constantly motivating me and all of the moral support. And last, but certainly not least, my parents. Without their continuous sacrifices, it was impossible for me to continue my research in Canada. Being the single child in the family, it has been hard for me stay away from them. I just want to let them know that whatever I have achieved in my life or will in the near future , it is built on all of their sacrifices and love.

To...

My parents, Altaf Hossain & Nasima Pervin for giving me the thinking space and teaching me the valuable lessons in life.

Table of Contents

List of Tables

List of Figures

Abbreviations

ANN Artificial Neural Network.

BERT Bidirectional Encoder Representations from Transformers.

CDF Cumulative Distribution Function.

CNN Convolutional Neural Network.

CNS Central Nervious System.

CPU Central Processing Unit.

dFC Dynamic Functional Connectivity.

DTI Diffusion Tensor Imaging.

EC Effective Connectivity.

EEG Electroencephalogram.

FA Fractional Anisotropy.

FC Functional Connectivity.

FCF Functional Connectome Fingerprinting.

FWHM Full-Width at Half Maximum.

GAN Generative Adversarial Network.

GCN Graph Convolutional Network.

GPU Graphics Processing Unit.

GRU Gated Recurrent Unit.

ICA Independent Component Analysis.

IQR Interquartile Range.

MD Mean Diffusivity.

MEG Magnetoencephalography.

MRI Magnetic Resonance Imaging.

MSE Mean Squared Error.

NIBS Non-Invasive Brain Stimulation.

NMI Normalized Mutual Information.

PCA Principal Component Analysis.

PDF Probability Distribution Function.

PFCF Pairwise Functional Connectome Fingerprinting.

PGTC Participants Greater Than Chance.

PLS Partial Least Squares.

ReLU Rectified Linear Unit.

RMSProp Root Mean Squared Propagation.

RNN Recurrent Neural Network.

ROI Region Of Interest.

rs-fMRI Resting-State Functional Magnetic Resonance Imaging.

RSTC Resting State Temporal Correlations.

SC Structural Connectivity.

sFC Static Functional Connectivity.

SGD Stochastic Gradient Descent.

SIFT2 Spherical-deconvolution Informed Filtering of Tractograms 2.

SVD Singular Value Decomposition.

Chapter 1

Introduction

1.1 Thesis Organization

This thesis has been drafted using a manuscript style (sandwich) format, in accordance with the University of Manitoba Faculty of Graduate Studies guidelines [1]. The remainder of the first chapter (Chapter 1) provides a general background of the problem and introduces some of the key concepts and terminology that will be used in subsequent chapters. It also specifies regarding the primary motivation of the problem and how I aim to solve this and why I have chosen these specific techniques. Chapter 2 and Chapter 3 describe the two main bodies of work that were undertaken during the MSc project and have each been prepared in a manuscript format (to be submitted for publication in peer-reviewed journals). Chapter 2 describes the structural and functional MRI dataset that we have created, as well as the performance evaluation parameters that we will use to benchmark our proposed deep learning approach for predicting brain functional connectivity from structural connectivity. Chapter 3 compares a modification of the algorithms and its effects on the performance evaluation algorithm. Chapter 4 provides a general discussion, and future research directions.

1.2 Brain Connectivity

The complexity of any primate nervous system depends on the intricate morphology of the underlying structures. Earlier neuroanatomists have played a pivotal role in under-

[1] https://umanitoba.ca/graduate-studies/student-experience/thesis-and-practicum/format-your-thesis-or-practicum

standing different fundamental properties of the nervous systems. In a highly evolved nervous system such as the human central nervous system (CNS), neuroanatomical patterns can be understood at several scales (Sporns et al., 2000). At the highest macroscopic level, the CNS consists of the brain and spinal cord, and the brain is subdivided into two hemispheres (right and left) that each contain four lobes – i.e., the frontal lobe, parietal lobe, temporal lobe, and occipital lobe (Kandel et al., 2000). At the microscopic cellular level, brain tissues are composed of various cell types, most notably various types of neurons and glia and at the sub-cellular level, neurons themselves are composed of soma (the main cell body), axons (projections that send signals to other neurons), and dendrites (projections that receive signals from other neurons) (Dayan & Abbott, 2005; Kandel et al., 2000) and the interfaces/connections between axons and dendrites are known as synapses. Panning back out from the microscopic to the macroscopic level, the brain can be thought of as a large, interconnected mesh, with pathways linking specific portions of cerebral cortex. The exact numbers vary from person to person, and change throughout the lifespan with age, but to give some perspective, a typical adult human brain weighs approximately 1300 grams, contains approximately 86 billion neurons (Herculano-Houzel, 2009) and is estimated to have between 100 to 500 trillion synapses (Drachman, 2005).

In general, brain tissues are commonly sub-divided (based on their appearance) into two different classes: gray matter and white matter. Gray matter makes up the outer most layer of the brain and its gray tones from the high concentration of neuronal cell bodies that it contains (Kandel et al., 2000). White matter lies beneath the the outermost layer of the brain's gray matter , and consists of millions of bundles of axons (nerve fibers) that connect neurons in different brain regions into functional circuits. The white color derives from a form of electochemical insulation (myelin) that coats axons (Kandel et al., 2000) which is formed by nonneuronal cells a form of electochemical called oligodendrocytes (Fields, 2010).

Human brain connectivity refers to the anatomical links (structural connectivity), or statistical dependencies (functional connectivity) or causal interactions (effective

connectivity) between distinct units within a nervous system. In connectivity literature, the so called "unit" consists of individual neurons, neuronal populations or anatomically parcellated brain sections. Brain connectivity patterns can be formed by structural links via fiber pathways and synapses, or by functional temporal relationships measured in terms of coordinated neural activity between parcellated regions (Sporns, 2007).

From the beginning of the 19th century, the method for dividing the central nervous system into discrete regions has been a matter of study and debate (Rushmore et al., 2020). From the regional organization perspective, the human brain has been extensively described using post-mortem material and is generally agreed upon. Although gross anatomical and histological features have been well studied in the human brain, precise knowledge of brain connections between specific areas, from origins to terminations, is more limited. This has been the case since the classic neuroanatomical studies of the 19th century (Rushmore et al., 2020). On the other hand, experimental neuroscientists have focused more on brain connection through brain organization rather than its clinical relevance. This research has used invasive methods that provide a high level of microscopic detail and employ systematic methodologies aimed at charting connections (Gallyas et al., 1980; Nauta & Ebbesson, 2012).

Later, this line of investigation continues using non-invasive brain imaging techniques such as magnetic resonance imaging or MRI (specifically diffusion MRI and functional MRI), Non-Invasive Brain Stimulation (NIBS), Electroencephalogram (EEG), and Magnetoencephalography (MEG) can provide in vivo data (Rushmore et al., 2020). In recent times, brain anatomical and functional organizations are evaluated from the perspective of complex brain networks (Bassett et al., 2018; Bullmore & Sporns, 2009; Sporns, 2011) and needed new terminologies to define these complex mechanisms. The connectome is the complete description of the physical wiring of an organism's nervous system which describes the comprehensive set of neuronal connections of a species CNS. Discovering the network characteristics of the human macroscale connectomes can direct scientists to the different morphological functions in the brain (Ardesch et

al., 2019; Sporns, 2016). The main idea of these brain networks is to classify neuronal networks with a small number of neurobiologically meaningful and easily computable measures and creating connectome for individual connectivity.

1.2.1 Structural Connectivity

Structural Connectivity or SC is the anatomical connectivity between different regions of the brain. SC is commonly measured using diffusion tensor imaging (DTI). The main idea is to capture the diffusivity of water molecules in the brain, since the mobility of water is restricted perpendicular to the axons oriented along the fiber tracts, thus capturing the white matter tracts in the brain. As diffusion differs between different tissue types of the brain, these techniques are suitable for evaluating white matter tissue characteristics. Various procedures are used to compute the white matter integrity such as: fractional anisotropy (FA), mean diffusivity (MD), fiber count and probabilistic tractography (Damoiseaux & Greicius, 2009). Through the analysis of the structural contributions of individual areas, researchers can identify and classify network hubs, defined as highly connected and highly central brain regions, which include areas of parietal and prefrontal cortex. The use of non-invasive diffusion imaging methodologies has opened new and promising avenues towards achieving this important goal. A detailed version of the morphological connection is described in Chapter 2.

1.2.2 Functional Connectivity

With the development of electrophysiology and the discovery of electrical activity of neurons, it was identified that through action potentials, transmission of signals are propagated through neurons. These activities were commonly studied using electrophysiological methods (invasive electrodes and non-invasive EEG). After the invention of functional MRI or fMRI, scientists started using fMRI for measuring and mapping the brain's functional activities such as speech or listening. Blood oxygenation level dependent (BOLD) fMRI measures spatiotemporal changes in blood flow and oxygenation that occurs in the brain due to hemodynamic response to a altered (in-

creased or decreased) neural activity. By examining the BOLD signal changes in different regions of the brain, scientists can infer different distinct properties of the brain (Glover, 2011). Functional connectivity indicates the statistical relationship between specific physiological signals in time and are generally evaluated using techniques such as functional magnetic resonance imaging (fMRI), electroencephalography (EEG) or magnetic electroencephalography (MEG) (Ellenbroek & Youn, 2016). For the context of this study, we will be focusing on the functional connectivity using fMRI. In general, functional connectivity calculates the deviations from statistical independence between distributed and often spatially remote neuronal units. Statistical dependence may be assessed by calculating correlation or covariance, spectral coherence, or phase-locking. It may be observed that FC is often calculated between all elements of the unit, regardless of whether these elements are connected by direct structural links. It should be noted that FC does not make any explicit reference to specific directional effects or to an underlying structural model (Sporns, 2007). Further information regarding the preprocessing of functional connectivity is available in Chapter 2.

1.2.3 Relationship Between Structural Connectivity & Functional Connectivity

Earlier studies have reported that SC and FC are strongly correlated in different regions such as: adjacent cortical regions (Koch et al., 2002), across 66 regions of the cerebral cortex (Hagmann et al., 2008). Using DTI and resting state temporal correlations (RSTC), researchers have showed significant agreement between these two types of connectivity in the overall architecture (Skudlarski et al., 2008). Beyond the analysis of empirical correlations between SC and FC, computational models have been used extensively to investigate the relationships between SC-FC (Messé et al., 2015). One of the seminal studies (Honey et al., 2009) in recent times demonstrated that using the computational models for brain SC-FC prediction, researchers were able to identify strong functional connections between regions with no direct structural connections; suggesting that many functional connections are formed in the absence of a direct structural connection. Researchers (Mišić et al., 2016) have also experimented

with a multivariate statistical technique to observe that connections between SC-FC. Their findings suggest that SC, FC do not show a one-to-one correspondence between structural and functional edges, suggesting these relationships are distributed and heterogeneous, with many functional relationships arising from non-overlapping sets of anatomical connections. Previous researchers mostly focused on the problem from the perspective of group-averaged matrices of SC and FC rather than subject specific correlations. One of the recent studies (Zimmermann et al., 2018) focused on the problem of individual subject specific SC-FC relationship in a standardized dataset and reported that the specificity of this SC-FC relationship was not unique to an individual despite having a correlation between group-averaged SC-FC.

As stated from the earlier discussion, many of the physiological mechanisms cannot be directly inferred from the existing techniques of analysis. These limitations have motivated researchers to apply different data-driven approaches, such as Partial Least Squares (PLS) (Mišić et al., 2016) and multivariate statistical techniques such as Principal Component Analysis (PCA), Independent Component Analysis (ICA) for investigating the relationships (Lin et al., 2021; McIntosh & Mišić, 2013). Even researchers have tried with computational models to predict FC from SC (Messé et al., 2015) but observed that there lies little impact on these model's predictive power of mapping out FC. We therefore theorize that for analyzing and predicting subject-specific FC connectivity matrices from their SC matrices, we will likely need to employ more advanced data-driven processing algorithms such as deep learning. Unlike classical machine learning algorithms, where users must handpick a set of features, deep learning algorithms could choose the features on its own. The following section provides a brief overview of machine learning and deep learning methods, and in particular; why we will focus on using the Graph CNN structures.

1.3 Deep Learning

Although the term Artificial Intelligence (AI) has become ubiquitous, it is difficult to pinpoint a singular definition. The authors (Russell & Norvig, 2022) addressed

the definition of AI from four potential goals or objectives of AI, which differentiate computer systems based on rationality and thinking vs acting on behalf. At its simplest form, artificial intelligence is a field, which combines computer science and robust datasets, to enable problem-solving. It also encompasses sub-fields of machine learning and deep learning, which are frequently mentioned in conjunction with artificial intelligence. Machine learning: a subset of AI is a method of data analysis which provides systems the ability to automatically learn and improve from data and experience without being explicitly programmed. It learns from the patterns of the data to build up a model which could simulate the learned parameters from unseen data. Depending on the task and the data, deep learning algorithms can be customized into numerous configurations. One of the most fundamental subdivisions can be supervised and unsupervised learning. In supervised machine learning the model learns the relationship between the labelled input and output data. However, labelled training data will often be resource intensive to utilize. Unsupervised machine learning on the other hand learns from unlabelled raw training data. An unsupervised model will learn relationships and patterns within this unlabelled dataset, so is often used to discover intrinsic characteristics in each dataset. In reinforcement learning, the objective of the algorithm is to learn from the environment through trial and error while optimizing some objective function. So, based on different purposes and objectives, different machine learning models are applied to solve the problem.

The main purpose of machine learning is to create mathematical models that can be trained to produce meaningful outputs (depending on the task) when input data is fed to the mathematical model. Traditionally, machine learning models are trained to perform useful tasks based on manually designed features extracted from the data, or features learned by other simple machine learning models. This feature representation can range from the attributes of the datasets to the customized features of the dataset. Let us think about an example of a famous machine learning models such as Artificial Neural Network (ANN). Usually, any ANN consists of several connected computational units sequentially. These computation units are named as neurons (as the design is

inspired by the biological networks of neurons in the human brain (Ackley et al., 1985; Lake et al., 2017; Rumelhart et al., 1986)). The experimental data is fed into a connected layer known as the input layer, followed by hidden layers which transforms the data as it flows through. At the end, depending on the output attributes, the data goes through the output layer and produces the predicted result. This process is done several times through a particular subset of the dataset known as the training set. The model's generalization ability is generally estimated during these training phases, a validation set is used to further tune the model for appropriate configurations. After several iterations of training and tuning, the final model is evaluated on a test set, used to simulate how the model will perform when faced with new, unseen data. In any basic form of ANN, the following objective function,

$$y = f(x; \theta)$$

which attempts to map output y using the input data x and parameters of the model θ. The non-linear transformation of the neural network can be written as

$$f(x) = (f_1, f_2 \dots f_k)(x)$$

Here each element f_k is called a network layer (consists of mathematical transformation) which can be written as

$$f_k = \sigma_k(\theta_k f_{k\text{-}1})$$

σ_k are known as the activation functions which are used to impose non-linearity in the transformation,θ_k are the matrices of numbers, called the model's weights. The learning phase of the algorithms is known as the training. During the training phase, the model is fed training data and tasked with optimizing a specific objective. Depending on the objective, a deep learning algorithm can be trained using a different set of optimization methods and gradient based optimization is most common (Messé et al., 2015). During the training phase, the model is fed training data and tasked with optimizing specific objective. As a part of the optimization algorithm, the error for the current state of the model must be estimated and depending on the error, the model

needs to optimize its parameters (such as weights and biases). The error is known as the loss function. Depending on the different task (classification/regression), the loss function varies. In the case of classification, we are predicting output from a set of finite categorical values, using loss function like categorical cross entropy or hinge loss. For regression, we want to predict a continuous value from the given parameters using loss function such as mean square error or mean absolute error. The main objective of the operation is to learn how to best utilize the intermediate representations to form a complex hierarchical representation of the input (Rumelhart et al., 1986). The basic algorithm behind training neural networks can be summarized as follows: training data is fed through the network, compute the gradient of the loss function with respect to every weight using the chain rule, and reduce the loss by changing these weights using optimization algorithm.

Deep learning is a subfield of machine learning that transforms the input successively to different representations in a layered fashion, which can later be used to produce the output depending on the task (Bishop et al., 1995; LeCun et al., 2015). One of the main attributes of deep learning over machine learning is its ability to learn feature representation. There is a strong resemblance between how a human decides about a particular thing and how a deep learning algorithm learns (Lake et al., 2017; Nielsen, 2015; Russell & Norvig, 2022; Sejnowski, 2020). The concept of automated learning algorithms was not new; in fact, scientists began experimenting with the core ideas in the 1960's (Marvin & Seymour, 1969) and gradually progressed on the concepts on multilayer networks (Sejnowski, 2020) and back propagation (Rumelhart et al., 1986). However, in recent time, the progress of deep learning (both in theory and application) is pervasive in every aspect of modern life. The reason can be addressed as follows (a) the technological advances in high tech central processing unit (CPU) and graphics processing unit (GPU) (b) the availability of huge amount of data (Chen et al., 2020; Deng et al., 2009; Irvin et al., 2019; Puri et al., 2021) and (c) the development of efficient algorithms (Ioffe & Szegedy, 2015; Nair & Hinton, 2010; Srivastava et al., 2014; Vincent et al., 2010). These innovations were boosted when the 2012 large scale

ImageNet image categorization challenge was dominated by the Convolution Neural Network (Krizhevsky et al., 2012). After that, almost each domain in science and technology began experimenting with their curated dataset and novel algorithms to solve their problems through deep learning-based solution. This phenomenon gives us some of fascinating algorithms to apply on different domains as well. An exhaustive review of various deep learning architectures currently in use is beyond the scope of this thesis. However, a brief review of some of the representative architectures is given as a Table 1.1 at the end of this chapter.

Due to its structure, deep learning models require a lot of data to process the learning phase. Depending on the tasks to solve, different modification of the network architecture is implied. The classification problem is when a model is used to classify whether a certain data belongs to a known group. The model learns the relationship between input and output pair through training with the labeled dataset. In broad aspect of images, classification can be implemented on the entire image, or it can be on the individual pixels of an image (that can be considered as a segmentation problem). In case of a design perspective of a classification model, if the model's input is a collection of numbers as features, it can be best suited to use a fully connected neural network with the modifications of neural network parameters according to the task (Krizhevsky et al., 2012; Wang et al., 2020). In case of a classification based on the image, a convolution neural network (CNN) with adjacent fully connected layer would perform better (Krizhevsky et al., 2012). CNNs are a class of neural architectures designed specifically to better utilize spatial and configural information by taking 2D or 3D images as input (LeCun et al., 1998). Structurally, CNNs have convolutional layers interspersed with pooling layers, followed by fully connected layers similar to standard multilayer neural network. The role of a convolutional layer is to detect local features at different positions in the input feature maps with learnable weights and biases. Depending on the task at hand, convolution layer can extract feature (convolution layer), or up sample the latent feature space (transposed convolution) or simple linear function between input and the output. The extracted features are stored

as a feature maps which are trainable parameters. Structurally, a pooling layer follows a convolutional layer to down-sample the feature maps of the preceding convolutional layer by taking the maximum (max pooling), average (avg pooling) or to up-sample the feature maps (un-pooling). Specifically, each feature map in a pooling layer is linked to a feature map in the convolutional layer; each unit in a feature map of the pooling layer is computed based on a subset of units within a local receptive field from the corresponding convolutional feature map (Shen et al., 2017). Normalization helps to limit the unbound activation in the previous layers which can be trainable. Activation functions (such as ReLU, Tanh) introduces non-linearity so that the CNN can map complex features. The loss is calculated as the difference between the input and proposed output and the CNN tries to optimize the objective through optimization techniques such as SGD or RMSProp. Details can be observed from the Figure1.1.

If the input is a sequential data (such as text, time series data), the choice of the network architecture would be a Recurrent Neural Network (RNN), Long Short-Term Memory (LSTM) or Gated Recurrent Unit (GRU) (Deng et al., 2009; Young et al., 2018). Regression is commonly used as the process for a machine learning model to predict continuous outcomes. It can be used in several aspects as well. For example, Segmentation is an important first step in various image processing and biomedical imaging applications. Segmentation involves dividing the image into regions to separate distinct parts or objects and the task is to predict specific portions. Segmentation is typically framed as a pixel-wise classification problem in supervised learning setting. In that case, U-Net based structures (Ronneberger et al., 2015) is one of the most common (or widely used) architecture used for segmentation problems. However, application of U-Net is not limited to segmentation. It can be used for any application that requires a matrix-to-matrix transformation.

In CNNs, the neighbourhood of interacting pixels is restricted to be rectangular and therefore CNNs fall short of modeling data in which the units (or nodes) can interact with neighboring nodes not necessarily defined over a rectangular grid. As a result, if the input has some inherent characteristics (such as graphical relationships between

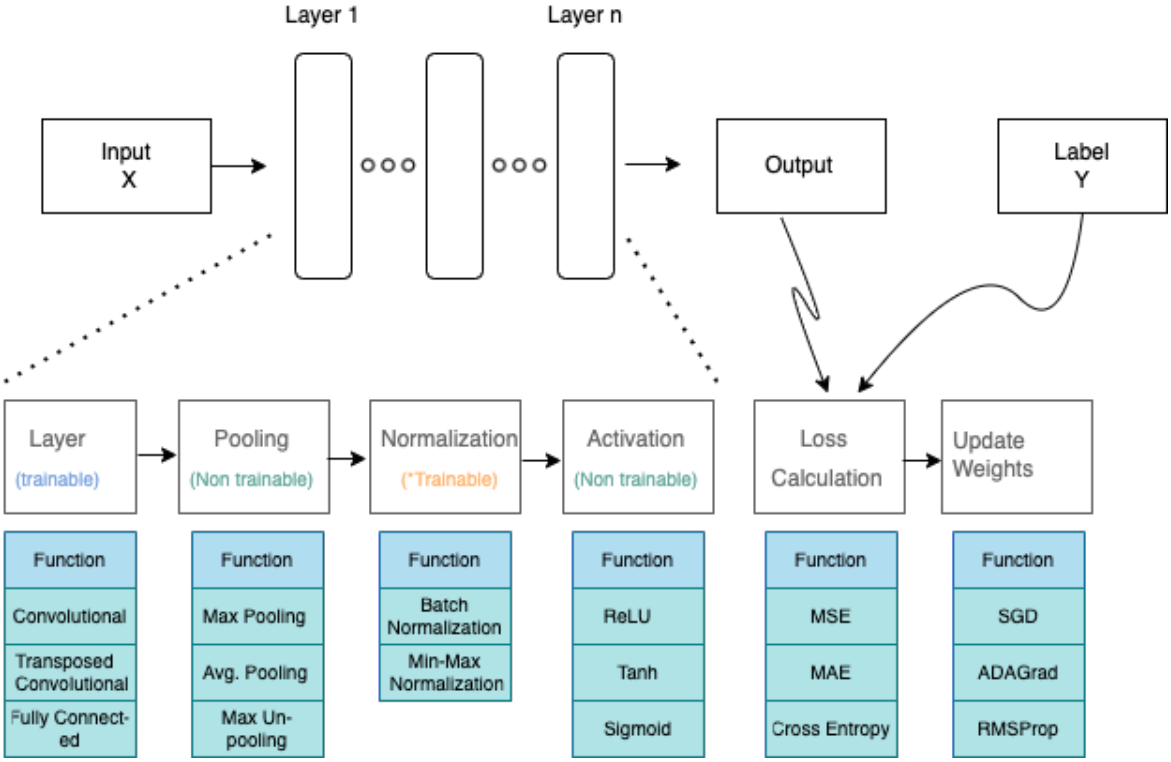

Figure 1.1: CNN and its all building blocks. The subordinate functions of each layer configurations are stacked under one another. At first, depending on the data processing pipelines, we take the features or up-sample it. Pooling layers reduces the dimension my taking maximum or average of the feature maps. Batch normalization helps to normalize the input before feeding it to another layer. Activation layers helps to introduce non-linearity. Using loss function such as MSE, a CNN optimize its learnable parameters through optimization techniques such as SGD, RMSProp.

structural units), graphical CNN based approach is more reasonable (Kipf & Welling, 2016) as compared to a traditional CNN.

In my case, the input, structural connectivity is a matrix with some inherent structures between each of the individual connectome parameters. The output is also a matrix of functional connectivity with inherent structures. I will be optimizing a supervised regression-based task using a U-Net based structures (Ronneberger et al., 2015) and a Graph Based CNN (Kipf & Welling, 2016).

1.4 Thesis Motivation

Previous studies have reported that SC and FC are strongly correlated (Honey et al., 2007; Honey et al., 2009), however there remains a gap in our understanding about

how these types of connectivities are related at the individual level. These limitations have motivated researchers to apply different data driven approaches, such as Singular Value Decomposition (SVD) (Zhan et al., 2015), Partial Least Squares (PLS) (Mišić et al., 2016) for investigating the relationships. Even researchers have tried with different computational models to predict FC from SC (Messé et al., 2015) but observed that there lies little impact on these models' predictive power of mapping out FC. Also, it is unclear how these modeling-based studies would support highly parcellated brain atlases with large numbers of brain regions Glasser (Glasser et al., 2016) in the high dimensional space to investigate subject specific SC to FC mapping through a data driven process for a high-quality data processing pipeline.

1.5 Thesis Objective

Based on the assumption that SC and FC are correlated, the overarching objective of the project was to develop, implement, and optimize a deep learning approach to predict/construct subject-specific FC connectomes from SC connectomes using a purely data driven process.

However, in order to achieve this aim, and to help future research in our group and others to do the same, we first identified two distinct objectives: 1) standard dataset accumulation and widely availability (making it open source, so that researchers can incorporate their algorithms in a similar manner); and 2) To identify and develop a standard set of performance metrics for evaluating AI-based SC-FC predictions.

Table 1.1: Summary of widely used deep learning architectures

Name of the architecture	**Short Description**
AlexNet (Krizhevsky et al., 2012)	Consists of 5 Convolution layer and 3 Fully connected layers, with ReLu activation function. Total 62 million trainable parameters. Winner of the 2012 image net challenge
VGG Net (Simonyan & Zisserman, 2014)	Using multiple small kernels to reproduce the receptive field. Total 138 million trainable parameters.
Google Net (Szegedy et al., 2015)	Stacking the layers in CNN more densely using multiple different filter size. 6.4 Million parameters. Winner of 2014 Imagenet challenge.
ResNet (He et al., 2016)	Introduction of 'short-cut' between layers known as skip connection. Different number of trainable parameters depending on the structures. Resnet 152 have 60.3 million parameters.
YOLO (Redmon et al., 2016)	Introduces simplified way to simultaneous object detection and classification in images. It incorporates several elements from Google Net. Its fast enough for real time processing.
GAN (Goodfellow et al., 2014)	It consists of two networks (generative and discriminative) which learns in an adversarial manner. The generative network tries to create new sample and the discriminative network tries to classify it as the generative output. The network learns simultaneously while optimizing these objectives.
U-Net (Ronneberger et al., 2015)	Originally used for biomedical image segmentation. Using an up-sample and down-sample block and skip connection, it creates segmentation masks of the desired output.
Transformer (Vaswani et al., 2017)	Language model that learns context and thus meaning by tracking relationships in sequential data like the words in this sentence using encoder/decoder block.
BERT (Devlin et al., 2018)	Able to understand context just as the humans do, pre-trained on Wikipedia data.
RNN (Rumelhart et al., 1986)	Recurrent Neural Network, where the output of the previous step is fed as an input to the current step. Used mainly for sequence labelling and classification.
LSTM (Hochreiter & Schmidhuber, 1997)	Long Short-Term Memory, is a variety of recurrent neural networks (RNNs) that are capable of learning long-term dependencies, especially in sequence prediction problems.
GRU (Cho et al., 2014)	Gated Recurrent Unit, similar to LSTM but requires fewer parameters to train.

References

Ackley, D. H., Hinton, G. E., & Sejnowski, T. J. (1985). A learning algorithm for boltzmann machines. *Cognitive science*, *9*(1), 147–169.

Ardesch, D. J., Scholtens, L. H., & van den Heuvel, M. P. (2019). The human connectome from an evolutionary perspective. *Progress in brain research*, *250*, 129–151.

Bassett, D. S., Zurn, P., & Gold, J. I. (2018). On the nature and use of models in network neuroscience. *Nature Reviews Neuroscience*, *19*(9), 566–578.

Bishop, C. M. et al. (1995). *Neural networks for pattern recognition*. Oxford university press.

Bullmore, E., & Sporns, O. (2009). Complex brain networks: Graph theoretical analysis of structural and functional systems. *Nature reviews neuroscience*, *10*(3), 186–198.

Chen, H., Xie, W., Vedaldi, A., & Zisserman, A. (2020). Vggsound: A large-scale audio-visual dataset. *ICASSP 2020-2020 IEEE International Conference on Acoustics, Speech and Signal Processing (ICASSP)*, 721–725.

Cho, K., Van Merriënboer, B., Gulcehre, C., Bahdanau, D., Bougares, F., Schwenk, H., & Bengio, Y. (2014). Learning phrase representations using rnn encoder-decoder for statistical machine translation. *arXiv preprint arXiv:1406.1078*.

Damoiseaux, J. S., & Greicius, M. D. (2009). Greater than the sum of its parts: A review of studies combining structural connectivity and resting-state functional connectivity. *Brain structure and function*, *213*(6), 525–533.

Dayan, P., & Abbott, L. F. (2005). *Theoretical neuroscience: Computational and mathematical modeling of neural systems*. MIT press.

Deng, J., Dong, W., Socher, R., Li, L.-J., Li, K., & Fei-Fei, L. (2009). Imagenet: A large-scale hierarchical image database. *2009 IEEE conference on computer vision and pattern recognition*, 248–255.

Devlin, J., Chang, M.-W., Lee, K., & Toutanova, K. (2018). Bert: Pre-training of deep bidirectional transformers for language understanding. *arXiv:1810.04805*.

Drachman, D. A. (2005). Do we have brain to spare? *Neurology*, *64*(12), 2004–2005.

Ellenbroek, B., & Youn, J. U. (2016). *Gene-environment interactions in psychiatry: Nature, nurture, neuroscience*. Academic Press.

Fields, R. D. (2010). Change in the brain's white matter. *Science*, *330*(6005), 768–769.

Gallyas, F., Zaborszky, L., & Wolff, J. (1980). Experimental studies of mechanisms involved in methods demonstrating axonal and terminal degeneration. *Stain technology*, *55*(5), 281–290.

Glasser, M. F., Coalson, T. S., Robinson, E. C., Hacker, C. D., Harwell, J., Yacoub, E., Ugurbil, K., Andersson, J., Beckmann, C. F., Jenkinson, M., et al. (2016). A multi-modal parcellation of human cerebral cortex. *Nature*, *536*(7615), 171–178.

Glover, G. H. (2011). Overview of functional magnetic resonance imaging. *Neurosurgery Clinics*, *22*(2), 133–139.

Goodfellow, I., Pouget-Abadie, J., Mirza, M., Xu, B., Warde-Farley, D., Ozair, S., Courville, A., & Bengio, Y. (2014). Generative adversarial nets. *Advances in neural information processing systems*, *27*.

Hagmann, P., Cammoun, L., Gigandet, X., Meuli, R., Honey, C. J., Wedeen, V. J., & Sporns, O. (2008). Mapping the structural core of human cerebral cortex. *PLoS biology*, *6*(7), e159.

He, K., Zhang, X., Ren, S., & Sun, J. (2016). Deep residual learning for image recognition. *Proceedings of the IEEE conference on computer vision and pattern recognition*, 770–778.

Herculano-Houzel, S. (2009). The human brain in numbers: A linearly scaled-up primate brain. *Frontiers in human neuroscience*, 31.

Hochreiter, S., & Schmidhuber, J. (1997). Long short-term memory. *Neural computation*, *9*(8), 1735–1780.

Honey, C. J., Kötter, R., Breakspear, M., & Sporns, O. (2007). Network structure of cerebral cortex shapes functional connectivity on multiple time scales. *Proceedings of the National Academy of Sciences*, *104*(24), 10240–10245.

Honey, C. J., Sporns, O., Cammoun, L., Gigandet, X., Thiran, J.-P., Meuli, R., & Hagmann, P. (2009). Predicting human resting-state functional connectivity from structural connectivity. *Proceedings of the National Academy of Sciences*, *106*(6), 2035–2040.

Ioffe, S., & Szegedy, C. (2015). Batch normalization: Accelerating deep network training by reducing internal covariate shift. *International conference on machine learning*, 448–456.

Irvin, J., Rajpurkar, P., Ko, M., Yu, Y., Ciurea-Ilcus, S., Chute, C., Marklund, H., Haghgoo, B., Ball, R., Shpanskaya, K., et al. (2019). Chexpert: A large chest radiograph dataset with uncertainty labels and expert comparison. *Proceedings of the AAAI conference on artificial intelligence*, *33*(01), 590–597.

Kandel, E. R., Schwartz, J. H., Jessell, T. M., Siegelbaum, S., Hudspeth, A. J., Mack, S., et al. (2000). *Principles of neural science* (Vol. 4). McGraw-hill New York.

Kipf, T. N., & Welling, M. (2016). Semi-supervised classification with graph convolutional networks. *arXiv preprint arXiv:1609.02907*.

Koch, M. A., Norris, D. G., & Hund-Georgiadis, M. (2002). An investigation of functional and anatomical connectivity using magnetic resonance imaging. *Neuroimage*, *16*(1), 241–250.

Krizhevsky, A., Sutskever, I., & Hinton, G. E. (2012). Imagenet classification with deep convolutional neural networks. *Advances in neural information processing systems*, *25*.

Lake, B. M., Ullman, T. D., Tenenbaum, J. B., & Gershman, S. J. (2017). Building machines that learn and think like people. *Behavioral and brain sciences*, *40*.

LeCun, Y., Bengio, Y., & Hinton, G. (2015). Deep learning. *nature*, *521*(7553), 436–444.

LeCun, Y., Bottou, L., Bengio, Y., & Haffner, P. (1998). Gradient-based learning applied to document recognition. *Proceedings of the IEEE*, *86*(11), 2278–2324.

Lin, Y., Ma, J., Huang, B., Zhang, J., Zhang, Y., & Dai, Z. (2021). Predicting human intrinsic functional connectivity from structural connectivity: An artificial neural network approach. *IEEE Transactions on Network Science and Engineering*, *8*(3), 2625–2638.

Marvin, M., & Seymour, A. P. (1969). Perceptrons. *Cambridge, MA: MIT Press*, *6*, 318–362.

McIntosh, A. R., & Mišić, B. (2013). Multivariate statistical analyses for neuroimaging data. *Annual review of psychology*, *64*, 499–525.

Messé, A., Rudrauf, D., Giron, A., & Marrelec, G. (2015). Predicting functional connectivity from structural connectivity via computational models using mri: An extensive comparison study. *NeuroImage*, *111*, 65–75.

Mišić, B., Betzel, R. F., De Reus, M. A., Van Den Heuvel, M. P., Berman, M. G., McIntosh, A. R., & Sporns, O. (2016). Network-level structure-function relationships in human neocortex. *Cerebral Cortex*, *26*(7), 3285–3296.

Nair, V., & Hinton, G. E. (2010). Rectified linear units improve restricted boltzmann machines. *Icml*.

Nauta, W. J., & Ebbesson, S. O. (2012). *Contemporary research methods in neuroanatomy: Proceedings of an international conference held at the laboratory of perinatal physiology, san juan, puerto rico, in january 1969 under the auspices of the national institute of neurological diseases and stroke and the university of puerto rico*. Springer Science & Business Media.

Nielsen, M. A. (2015). *Neural networks and deep learning* (Vol. 25). Determination press San Francisco, CA, USA.

Puri, R., Kung, D. S., Janssen, G., Zhang, W., Domeniconi, G., Zolotov, V., Dolby, J., Chen, J., Choudhury, M., Decker, L., et al. (2021). Codenet: A large-scale ai for code dataset for learning a diversity of coding tasks. *arXiv preprint arXiv:2105.12655*.

Redmon, J., Divvala, S., Girshick, R., & Farhadi, A. (2016). You only look once: Unified, real-time object detection. *Proceedings of the IEEE conference on computer vision and pattern recognition*, 779–788.

Ronneberger, O., Fischer, P., & Brox, T. (2015). U-net: Convolutional networks for biomedical image segmentation. *International Conference on Medical image computing and computer-assisted intervention*, 234–241.

Rumelhart, D. E., Hinton, G. E., & Williams, R. J. (1986). Learning representations by back-propagating errors. *nature*, *323*(6088), 533–536.

Rushmore, R. J., Bouix, S., Kubicki, M., Rathi, Y., Yeterian, E. H., & Makris, N. (2020). How human is human connectional neuroanatomy? *Frontiers in Neuroanatomy*, *14*, 18.

Russell, S., & Norvig, P. (2022). *Artificial intelligence: A modern approach. 4th*. Pearson.

Sejnowski, T. J. (2020). The unreasonable effectiveness of deep learning in artificial intelligence. *Proceedings of the National Academy of Sciences*, *117*(48), 30033–30038.

Shen, D., Wu, G., & Suk, H.-I. (2017). Deep learning in medical image analysis. *Annual review of biomedical engineering*, *19*, 221.

Simonyan, K., & Zisserman, A. (2014). Very deep convolutional networks for large-scale image recognition. *arXiv preprint arXiv:1409.1556*.

Skudlarski, P., Jagannathan, K., Calhoun, V. D., Hampson, M., Skudlarska, B. A., & Pearlson, G. (2008). Measuring brain connectivity: Diffusion tensor imaging validates resting state temporal correlations. *Neuroimage*, *43*(3), 554–561.

Sporns, O., Tononi, G., & Edelman, G. M. (2000). Connectivity and complexity: The relationship between neuroanatomy and brain dynamics. *Neural Networks*, *13*, 909–922. https://doi.org/10.1016/S0893-6080(00)00053-8

Sporns, O. (2007). Brain connectivity. *Scholarpedia*, *2*(10), 4695.

Sporns, O. (2011). The human connectome: A complex network. *Annals of the new York Academy of Sciences*, *1224*(1), 109–125.

Sporns, O. (2016). *Networks of the brain*. MIT press.

Srivastava, N., Hinton, G., Krizhevsky, A., Sutskever, I., & Salakhutdinov, R. (2014). Dropout: A simple way to prevent neural networks from overfitting. *The journal of machine learning research*, *15*(1), 1929–1958.

Szegedy, C., Liu, W., Jia, Y., Sermanet, P., Reed, S., Anguelov, D., Erhan, D., Vanhoucke, V., & Rabinovich, A. (2015). Going deeper with convolutions. *Proceedings of the IEEE conference on computer vision and pattern recognition*, 1–9.

Vaswani, A., Shazeer, N., Parmar, N., Uszkoreit, J., Jones, L., Gomez, A. N., Kaiser, Ł., & Polosukhin, I. (2017). Attention is all you need. *Advances in neural information processing systems*, *30*.

Vincent, P., Larochelle, H., Lajoie, I., Bengio, Y., Manzagol, P.-A., & Bottou, L. (2010). Stacked denoising autoencoders: Learning useful representations in a deep network with a local denoising criterion. *Journal of machine learning research*, *11*(12).

Wang, H., Shi, H., Lin, K., Qin, C., Zhao, L., Huang, Y., & Liu, C. (2020). A high-precision arrhythmia classification method based on dual fully connected neural network. *Biomedical Signal Processing and Control*, *58*, 101874.

Young, T., Hazarika, D., Poria, S., & Cambria, E. (2018). Recent trends in deep learning based natural language processing. *ieee Computational intelligenCe magazine*, *13*(3), 55–75.

Zhan, L., Liu, Y., Wang, Y., Zhou, J., Jahanshad, N., Ye, J., Thompson, P. M., & (ADNI), A. D. N. I. (2015). Boosting brain connectome classification accuracy in alzheimer's disease using higher-order singular value decomposition. *Frontiers in neuroscience*, *9*, 257.

Zimmermann, J., Griffiths, J., Schirner, M., Ritter, P., & McIntosh, A. R. (2018). Subject specificity of the correlation between large-scale structural and functional connectivity. *Network Neuroscience*, *3*(1), 90–106.

Chapter 2

An open dataset and standardized performance evaluation parameters for comparing AI-based brain structural to functional connectome mapping

2.1 Abstract

Previous studies have shown that resting state functional connectivity (FC) can be predicted from structural connectivity (SC) through computational modelling and, more recently, data-driven artificial intelligence (AI) methods. With rapid advancements and with more wide-spread adoption, it is likely that deep learning and other AI methods will increasingly be used to elucidate (and predict) neural SC-FC relationships in both healthy and brain injury/disease populations. However, in order to evaluate how well different AI methods perform, without the confound of using different training and testing data, different SC and FC metrics, different image processing pipelines, and/or different brain atlases to segment the SC and FC connectomes, it would be useful to have an easily accessible open-access dataset that future studies can use. Furthermore, while different groups may opt to employ additional benchmarking methods of their choosing, it would be beneficial for future SC-FC studies to report a standardized set of performance metrics to enable direct comparisons between different AI methods. The objectives of this manuscript are therefore to: 1) describe and char-

acterize a publicly available dataset of subject-specific SC, mean FC, and dynamic FC connectomes based on diffusion and resting-state fMRI data from the Human Connectome Project (HCP) S900 release; 2) propose a set of minimum reporting guidelines for benchmarking subject-level SC-FC predictions, including a handful of well-established metrics that are used for evaluating AI performance, as well as a novel Pairwise Functional Connectome Fingerprinting (PFCF) approach that is of particular interest for this application; and 3) provide a practical example, using the proposed dataset and benchmarking metrics, by training/testing a graph convolutional network (GCN) to predict subject-specific FC matrices from subject-specific SC connectomes.

2.2 Introduction

Brain connectivity can refer to the anatomical links (structural connectivity; SC), temporal correlations in neural activity (functional connectivity; FC) or directional/ causal functional interactions (effective connectivity; EC) between different regions of the nervous system (Bullmore & Sporns, 2009; Park & Friston, 2013; Sporns, 2007). These measures of connectivity can be useful to better understand the cognitive functions and complex behaviors facilitated by the coordinated interactions between brain regions or networks (i.e., groups of structurally and/or functionally connected regions) (Bullmore & Sporns, 2012; Van Den Heuvel & Pol, 2010). Earlier modeling studies of brain connectivity (Honey et al., 2007; Honey et al., 2009) revealed underlying relationships between structural and functional connectivity; and more recent work has built on this using more complex modeling (Mišić et al., 2016) as well as Artificial Intelligence (AI) based methods (Kim et al., 2020; Y. Li et al., 2019; Neudorf et al., 2022; Sarwar et al., 2021; Zhang et al., 2020) to further investigate the relationships between brain SC and FC.

As AI driven algorithms become more abundant, more complex, and more commonly employed for this particular application, it will be increasingly important to quantify and compare the performance of different AI algorithms and their various implementations and settings. Moreover, because conventional regression-based

deep learning evaluation approaches (e.g., correlation coefficient, mutual information, mean squared error, etc.) do not necessarily provide context for the predictive accuracy relative to the underlying connectome data, and previous classification-based FC test/retest benchmarking approaches (e.g., Functional Connectome Fingerprinting (Finn et al., 2015)) have not been optimized to evaluate predictive performance over a potentially wide range (i.e., the likelihood of having at least one incorrect nearest-neighbor, which would produce a floor effect in an all-or-none classification metric), it is likely that an alternate classification-based method could be developed to provide meaningful results over a wider range, and therefore be better suited for such a challenging problem.

In the current paper, we therefore aimed to tackle these challenges by: 1) creating and curating a freely-available dataset of subject-specific SC and FC connectomes, based on the Human Connectome Project (HCP) S900 release; 2) characterizing the Pearson correlations (Corr), normalized mutual information (NMI), and mean squared error (MSE) between the measured SC and FC connectomes; and 3) proposing a novel classification benchmark called Pairwise Functional Connectome Fingerprinting (PFCF), which is based on the traditional Functional Connectome Fingerprinting (Finn et al., 2015), but evaluates classification performance over a wider range and is therefore a more suitable method for evaluating AI-based brain SC-FC predictions at the single subject level. Finally, using the aforementioned dataset and benchmarking parameters, we demonstrate a proof of concept to show how these can be employed and reported by implementing a recently proposed Graph Convolutional Network (GCN) (Y. Li et al., 2019) to predict individual subjects' FC based on their SC data.

2.3 Description of the Dataset

One of the main objectives of this project was to generate and share a set of open-access subject-specific SC, mean FC, and dynamic FC connectomes to facilitate standardization and enable direct comparisons to be made between future SC-FC studies. To this end, we used diffusion magnetic resonance imaging (dMRI) and resting-state func-

tional magnetic resonance imaging (rs-fMRI) data from the HCP S900 release (Van Essen et al., 2013) for 762[1] subjects. Segmentation for all SC and FC connectomes were based on the Glasser atlas (Glasser et al., 2016), and consisted of 180 regions per hemisphere for a total of 360 regions of interest. Details can be observed from Figure 2.1A.

The dMRI and rs-fMRI data acquisition parameters for the HCP study have already been described in detail (Smith et al., 2013; Sotiropoulos et al., 2013) and the preprocessing pipelines for this dataset have also been previously reported in the "HCP Glasser" section of (Zimmermann et al., 2018). In summary, the dMRI data were run through the HCP minimal preprocessing pipeline with motion correction, eddy current correction, and intensity normalization (Glasser et al., 2016); probabilistic tractography was performed using the MRtrix software (Tournier et al., 2012); and subject-specific SC connectomes were derived by quantifying connected edges of the 360 Glasser atlas ROI pairs using the weighted streamline count (SIFT2) by cross-sectional area method (Smith et al., 2013).

Since four replicate rs-fMRI scans were acquired from each participant in the HCP protocol (each 1200 time points; 14.4 min with a 720ms repetition time), each of these were preprocessed using motion correction (i.e., 6 degree of freedom denoising), spatial smoothing (2mm Gaussian FWHM 3D kernel), intensity normalization, and spatial normalization to both the MNI152 and surface-based multimodal brain templates. The static FC connectome for each of the four rs-fMRI scans was initially calculated as the mean (temporal) bi-variate correlation between each ROI-ROI pair in the Glasser atlas, across the entire scan length of 1200 time points (Figure 2.1B). Then, the resulting four FC connectomes were averaged to compute a mean subject-specific static FC (sFC) matrix.

However, since computing resting state FC over such long time-scales does not capture higher-frequency temporal information, we also performed dynamic functional connectivity (dFC) analyses to capture potential increases and/or decreases in FC

[1]S900 release has a total 897 3T MR imaging data. We received the preprocessed data from the German group (Dr. Ritter) as 766. Among them, some were missing, and we ended up with 762.

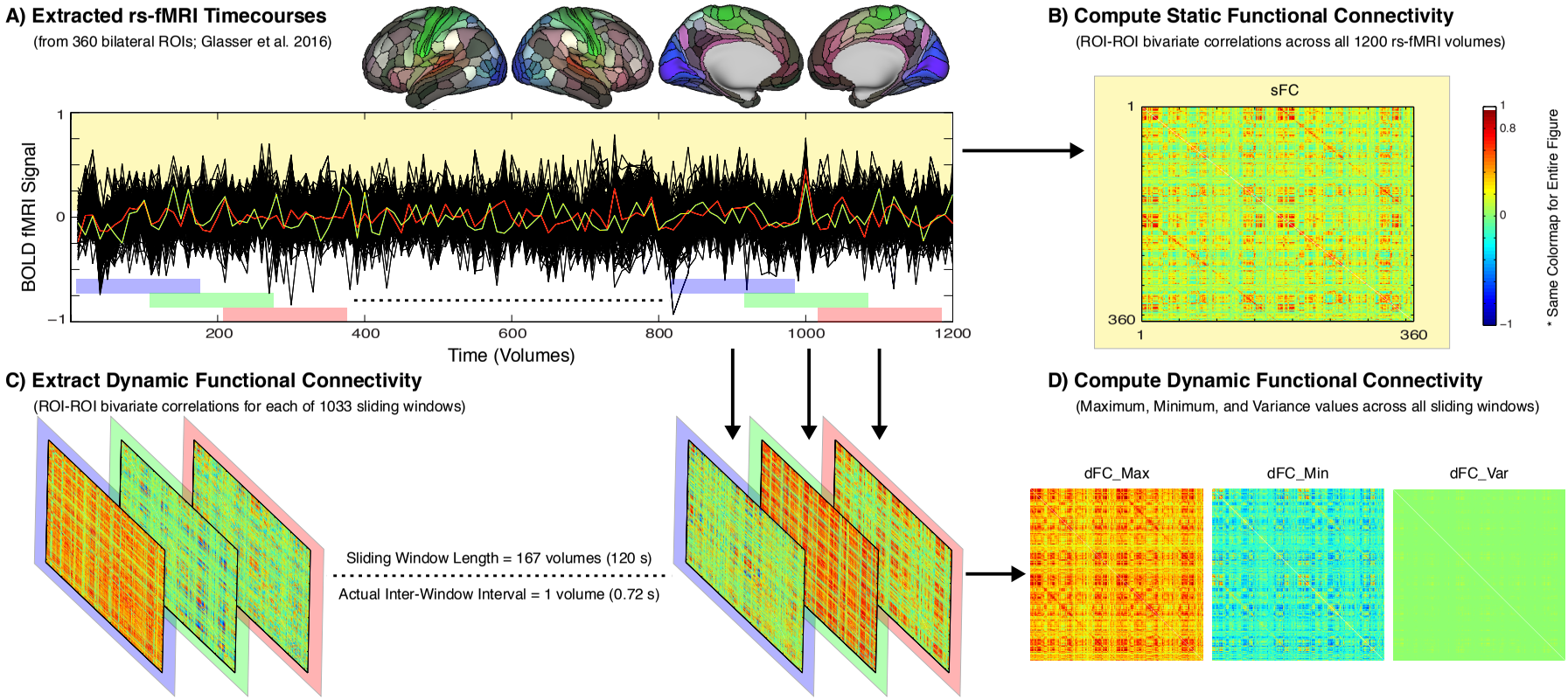

Figure 2.1: A) Extracted resting state fMRI of 1200 time points in total 14.4 mins. B) Using all those time points, Static Functional Connectivity was constructed with no overlapping windowed bi-variate correlations for each ROI-ROI pair across all four scans. C) Extract the dynamic connectivity from the time point analysis using a sliding window mechanism of 120s and 1033 windowed bi-variate correlations. D) And using those correlations, produce the maximum, minimum and variance of each ROI-ROI pair across all four scans.

over shorter timescales (Figure 2.1C). For this, we utilized a sliding window approach (Allen et al., 2014; Hutchison et al., 2013) to analyze each of the four rs-fMRI runs for each participant, employing a window length of 120s (i.e., 167 time points, given that rs-fMRI data were acquired with TR = 720ms), a step size of one (i.e., adjacent windows have 166 overlapping time points), and discarded endpoints (i.e., only returning values computed from full 167-element windows to produce 1200 - 167 = 1033 windowed bi-variate correlations for each ROI-ROI pair). Based on each of these 1033 windowed correlations, we extracted the maximum (dFC_Max), minimum (dFC_Min) and variance (dFC_Var) for each ROI-ROI pair within each of the four rs-fMRI runs, and these measures were then averaged across all four runs for each participant (Figure 2.1D). Although such a large window size sacrifices temporal resolution compared to shorter (e.g., 30s) windows, this is consistent with other theoretical work suggesting that the lower-bound for sliding window lengths ought to be 100s due to the fact that the lowest nominal resting state fMRI frequency is 0.01 Hz (Hutchison et al., 2013; Leonardi & Van De Ville, 2015). In our case, one of the empirical studies (Savva et al., 2019) have found that for statistical comparisons between other dataset, a window size of atleast 120s was deemed necessary for reproducing the results. That is why we chose to initialize our dataset's dynamic connectivity using a window length of 120s.

2.4 Availability of the Dataset

The entire dataset of subject-specific SC and FC connectomes described above is freely available to download from the Neuroimaging Tools & Resources Collaboratory (https://www.nitrc.org/; Note: we will create a NITRC tool/resource and insert the direct link here once the manuscript is accepted). The directory contains two parent folders: SC and FC. All of the subject-specific structural connectomes are organized in the SC folder according to their respective HCP Subject ID. The FC folder contains two sub-folders: one for the sFC connectomes, and one for the three dFC connectomes, where participants data are again organized according to respective HCP Subject ID. No subject-specific information, identifiable data, or identifiable metadata

are included in this release (only the aforementioned connectomes); however, by using the HCP Subject IDs, this data can be cross-referenced by investigators who have obtained the necessary ethics approval and been granted access to subject-specific data via the HCP investigators.

2.5 Characterizing Inter-Subject Differences In The Measured SC & FC Connectomes

The amount of inter-subject variability in the measured connectomes is likely to be an important factor for any future AI-based SC-FC (or FC-SC) predictions. Therefore, another objective of the study, after generating all of the subject-specific connectomes, was to determine the extent of inter-subject variability for each of the connectome types. To this end, we used Python 3 (Version 3.7 (Van & Drake, 2009)) to calculate the Corr, MSE, and NMI between each pair of participants, where Corr is the Pearson Correlation, MSE is the Mean Squared Error, and NMI is defined as Normalized Mutual Information which specifies a score to scale the results between 0 (no mutual information) and 1 (perfect correlation) (Shannon, 1949; Strehl & Ghosh, 2002). We also visualized these results using box and whisker plots (Figure 2.2), revealing at a glance that SC exhibited higher Corr, MSE, and NMI between participants compared to the measured sFC or dFC values, and also showed lower Corr-based variance and higher MSE-based variance.

2.6 Proposed Benchmarking/Performance Metrics For AI-based SC-FC Predictions

To facilitate direct comparisons between different SC-FC prediction studies (e.g., to determine the "best" deep learning method, "optimal" parameters, etc.), another one of the study's objectives was to propose a minimum set of performance evaluation parameters that can be used to benchmark different AI-based SC-FC (or FC-SC) predictions. In the next sections, we will discuss a handful of conventional statistical, introduce the concept Functional Connectome Fingerprinting (FCF; which is a rel-

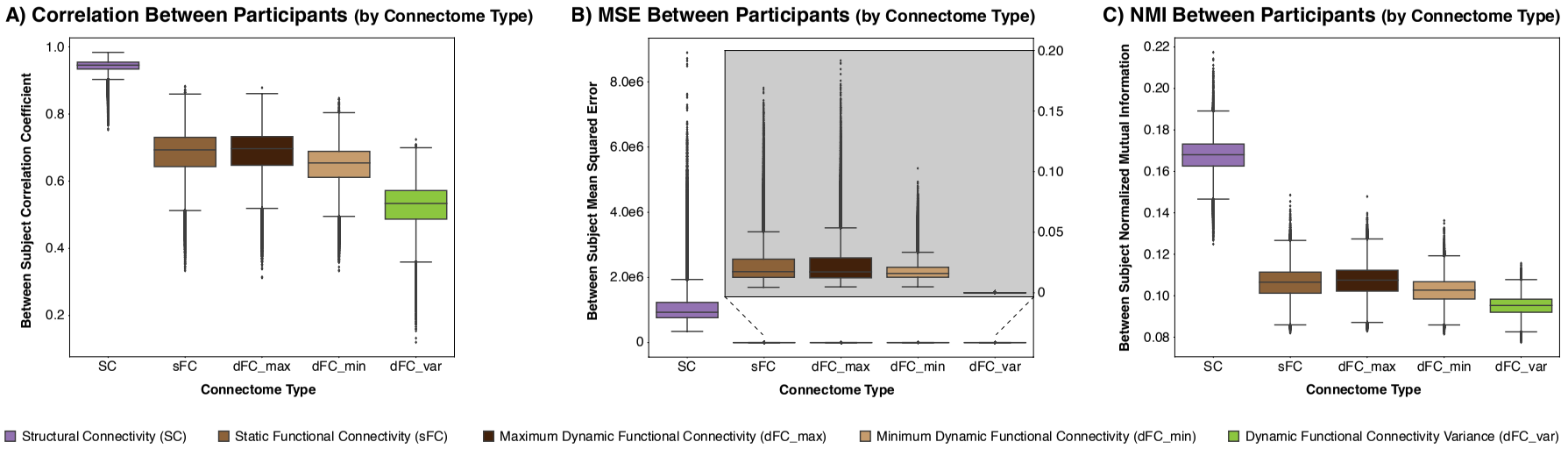

Figure 2.2: A) Measurement of similarity between participant's Structural Connectivity (SC), Static Functional Connectivity (sFC), Maximum Dynamic Functional Connectivity (dFC_Max), Minimum Dynamic Functional Connectivity (dFC_Min), Dynamic Functional Connectivity Varience (dFC_Var) calculated using A) Correlation Coefficient B) Mean Squared Error C) Normalized Mutual Information (NMI). In every scenario, the inter participant relationship between Structural Connectivity is always higher than other forms of connectivity

atively recent concept that has been gaining traction in the fMRI literature), and then introduce for a novel pairwise functional connectome fingerprinting performance metrics.

2.6.1 Conventional Computational Modeling and AI

To evaluate the result of group averaged SC-FC prediction, earlier studies focused on conventional benchmarking parameters, such as Pearson Correlations Coefficient (Corr) and Mean Squared Error (MSE) (Neudorf et al., 2022; Sarwar et al., 2021; Zimmermann et al., 2018). These parameters have the advantage of being quickly and easily computed, and are potentially useful for quantifying relative improvements between different models and/or parameters. For example, by comparing the values in a subject's predicted FC matrix to the corresponding values in their measured (ground truth) FC matrix, a model producing a higher Corr and lower MSE could be judged to be "better". Mutual information is another potentially useful information theoretic quantity that measures how much one random variable tells us about another, where more (higher) mutual information indicates a corresponding reduction in uncertainty. . It can be thought of as the reduction in uncertainty about one random variable given knowledge of another. Using these three statical methods, we proposed a series of comparison maps (more details in the result evaluation parameter section) and box and whisker plots for evaluating the AI-based results. However, while these three conventional methods are likely to serve as useful relative indicators of predictive performance, they are not absolute measures (other than perhaps the rare scenario of an exact match where MSE = 0; and where Corr and NMI would both necessarily equal 1, but where the opposite is not necessarily true).

2.6.2 Functional Connectome Fingerprinting Based Performance Parameters

As noted above, while conventional AI evaluation approaches (e.g., Corr and MSE) are useful to some extent for comparing outputs from different AI methods, they are relative measures that do not put the accuracy of the predicted FC output in

context (e.g., whether it was within the scale of naturally occurring variance between different subjects' measured FCs). Interestingly, recent work on test/re-test rs-fMRI data has demonstrated that FC matrices from individual subjects are highly consistent compared to the variability between different subjects, suggesting that any given FC matrix can serve as a unique subject identifier, similar to a "fingerprint" (Finn et al., 2015). Based on this, they proposed a method called Functional Connectome Fingerprinting (FCF), where they iteratively took each participant's FC matrix from an initial test dataset and compared it (using Corr) to the entire pool of participant FCs in the re-test dataset; and they demonstrated that participants' test and re-test FCs correctly matched themselves from within the entire pool of participants (lowest Corr) over (92.9% and 94.4% for two datasets) of the time. An interesting approach could therefore be used to benchmark the accuracies of predicted FCs from AI models (i.e., by comparing AI predicted FCs to the actual pool of measured FCs). However, the inherently difficult nature of predicting individual FC from SC – which is (at least in such early days) likely to generate predicted FCs that differ more from measured FCs than real-world test/retest rs-fMRI data – precludes simply adopting the existing FCF method (Finn et al., 2015) for this purpose.The problem is that choosing from the entire pool of measured FCs at once sets up an "all or none" scenario, where any predicted FC would be scored as a "failure" (i.e., failing to choose iteself) if there is even one measured FC producing a higher Corr, lower MSE, etc. (depending on the statistical parameter that we chose to evaluate our performance). That is potentially problematic because AI-based methods often predicts a generalized version of the connectivity and FCF could be prone to a floor effect.

2.6.3 A Novel Pairwise Functional Connectome Fingerprinting Performance Parameters

To work around the inherent all-or-none problem associated with the conventional FCF approach, one of the ideas could be to perform a series of pairwise comparison to increase the bandwidth of the result. With this motivation we propose the idea of Pairwise Functional Connectome Fingerprinting (PFCF), which is based on computing

the overall accuracy of the methods using a series of pairwise tests. This is based on the same principle as the conventional FCF approach, but instead of comparing one subject's predicted FC to the entire pool of measured participant FC's (one vs all), we can simply run a series of pairwise tests (using each subject's measured FC iteratively paired with every other subject's measured FC) and count how often it can classify itself from the series of tests. A logical counter is used to track the successful classifications among the whole operation. Depending upon the choice of comparison metrics (e.g, Corr, NMI, MSE), the PFCF accuracy for the j^{th} participant in the set of N participants is given as:

$$PFCF_{j(Metric)} = \frac{1}{N-1} \sum_{i=1, i \neq j}^{N} \delta(r_{Metric} Metric(\widehat{FC}_i - FC_j) > r_{Metric} Metric(\widehat{FC}_i - FC_i))$$

where

$$Metric\, \varepsilon\, \{Corr, MSE, NMI\}$$

FC_x= Measured FC of participant X, $\widehat{FC}_\text{x}$=Predicted FC of participant X and

$$r_{Metric} = \left\{ \begin{array}{c} +1, if Metric\, \epsilon\, \{Corr, NMI\} \\ -1, if Metric = MSE \end{array} \right\}$$

$\delta(Condition)$ is an indication function which evaluates to 1 if the condition (passed as an argument) is true and 0 otherwise. The overall PFCF accuracy corresponding to a metric is given by the following equation:

$$PFCF_{Accuracy(Metric)} = \frac{1}{N} \sum_{j=1}^{N} PFCF_{j(Metric)}$$

Conceptually, for any participant's predicted FC that is able to classify itself from the series of paired tests every time, the PFCF would score a 100% accuracy (i.e., the same as scoring 100% based on conventional FCF). Similarly, if it fails to correctly classify every time, PFCF accuracy would be 0% (i.e., the same as scoring 0% based on conventional FCF). Therefore, while PFCF is conceptually similar and captures the same overall performance bandwidth (0-100%) as conventional FCF, it has the advantage of overcoming the nearest-neighbor problem to offer more fine-grained intermediate

performance stratification - likely rendering it more suitable to characterizing the performance of AI-predicted FC connectomes. approximation of the analysis from the series of pairwise test that FCF cannot provide. The details of the procedure as well as an example of the process is described in the subsequent section of connectome fingerprinting analysis.

2.7 Proof-of-Principle: Implementing Subject-Specific FC Prediction Based on SC Data & GCN

For the scope of this article, we will focus our analysis only on mapping the static functional connectivity (sFC) from structural connectivity (SC), and the results will be reported using our proposed benchmarking parameters. The following sections describe the architecture of the specific neural network that we employed for the task of learning SC-sFC mapping: namely, a Graph Convolutional Network (Kipf & Welling, 2016).

2.7.1 Graph CNN

From a general point of view, a set of data can be represented into several aspects: each with its own added advantage. One of the advantages of deep learning is that the analysis can capture the hidden patterns between the data. The main motivation for adopting to graph based neural network architecture is to compensate for the complex relationship between the data and modelling parameters. The reason for analyzing with graph structure is that, both the brain structural and functional connectivity can be represented in the form of graphs; where the different connectomes act as the nodes and the connection strength between each of the nodes acts as the edge weight of the graph.

We implemented the Graph CNN from (Y. Li et al., 2019) with some modification (details can be observed from Figure 2.3). The architecture can be subdivided into three different parts: preprocessing, an encoder and a decoder. The preprocessing part makes the data compatible for the encoder and decoder. In the preprocessing step,

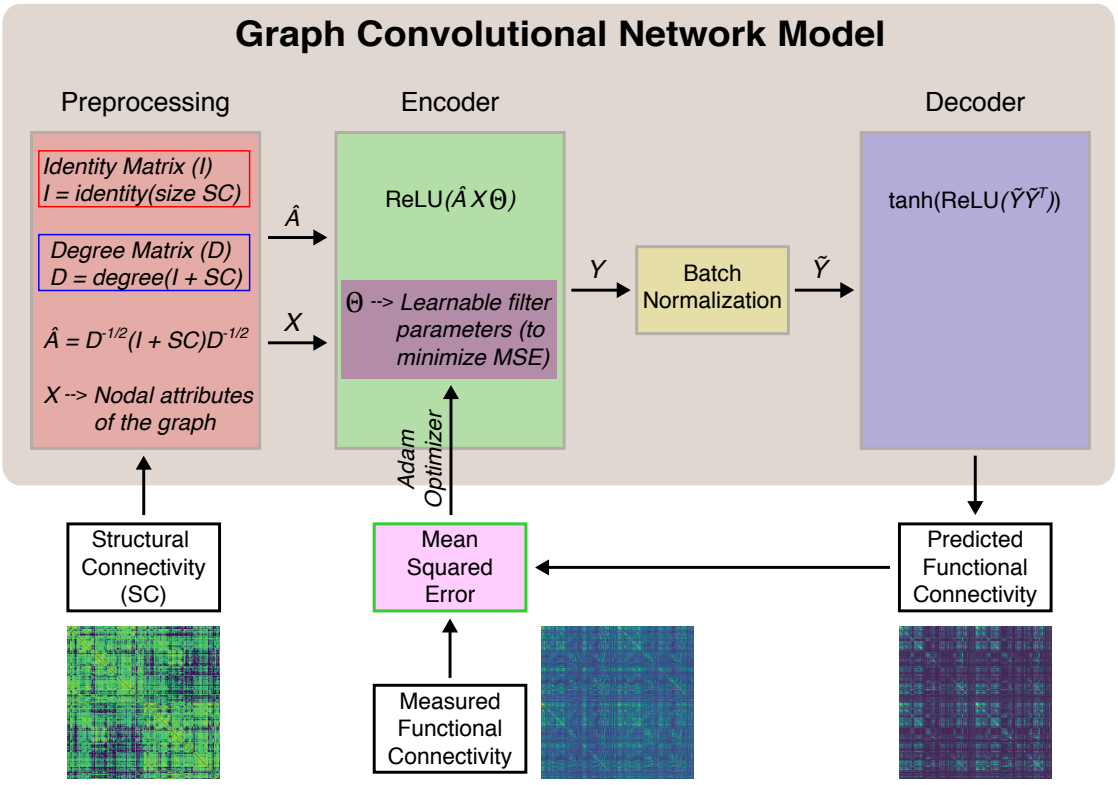

Figure 2.3: GCN for obtaining predicted FC from SC. The input of the network was preprocessed into degree and identity matrix of SC and fed to the encoder layer. X stands for the nodal attributes of the graph (specifically the node ids). The weight parameters are being updated with the convolution layer filter coefficients. Through Batch Normalization and Decoder, the model predicted output. MSE is used as a loss function to configure the weight of the model over 1000 epochs with a learning rate of 0.001.

the input SC is transformed into an adjacency matrix $\hat{A}$ where

$$\widehat{A} := \tilde{D}^{\frac{-1}{2}} \tilde{A} \tilde{D}^{\frac{-1}{2}}$$

$\tilde{D}$ is the degree matrix of the $\tilde{A}$ and

$$\tilde{A} = I + A$$

I is the identity matrix of the input A. For the encoder part, a single layer Graph CNN can be constructed as

$$E = ReLU(\widehat{A} X \theta)$$

where, ReLU stands for Rectified Linier Unit and can be written as ReLU(P) = max(0,P). X stands for the nodal attributes of the graph. The nodal attributes can

consist of any number of features, however, for this study we have used a one-hot representation for each node only to have the notion of each node being identifiable distinctly. That is why we chose $X \epsilon \mathbb{R}^{N \times K}$, where N is the number of nodes in the brain region (in our case its N=360), K is the nodal attributes (in our case, K = 360). The weight parameter θ is being updated with the convolution layer filter coefficients. It is defined as $\theta \epsilon \mathbb{R}^{K \times F}$; where F is number of filters in the convolution layer (since we are using a 360 based connectome, we chose the F=360). The configuration of K and F are based on our choice and for this experiment we make it similar to the number of regions in the connectome. The encoder matrix goes into to decoder layer, which can be defined as

$$Z = tanh(ReLU(EE^T))$$

Where $tanh(x) = \frac{e^x - e^{-x}}{e^x + e^{-x}}$. To ensure that no activation value of the encoder layer is too high or too low, a two-dimensional batch normalization is applied before going through the decoder's rectified linier unit activation. So, for the implementation of the Graph Encoder-Decoder based network, we took Structural Connectivity matrix as an input to learn how to map it to the Functional Connectivity. All 762 subjects were cross validated into 5-fold by portioning the dataset into 5 subsets. The distribution of training and testing was 80% for training and 20% for testing the performance. We used mean squared error (MSE) as the loss function where

$$MSE = \frac{1}{n} \sum_{i=1}^{n} (FC_{\text{measured}} - FC_{\text{predicted}})^2$$

n is the number of sample size. In each iteration, the model's weights and biases are updated based on the optimization technique. We used the Adam (Kingma & Ba, 2015) optimizer with a learning rate of 0.001. Each model is trained for 1000 epochs using Nvidia RTX-8000 GPU. The whole network was implemented in the Pytorch framework (Paszke et al., 2019).

2.7.2 Result Evaluation Parameters

After the model is trained successfully on each individual training fold, for validation the model was tested on the respective left-out test fold. Figure 2.4 shows side by

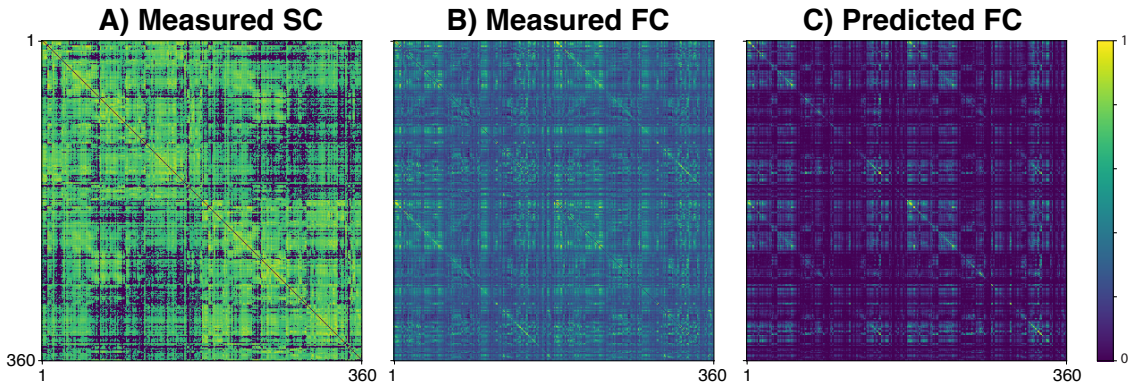

Figure 2.4: SC, Measured FC & Predicted FC connectomes for a randomly selected participant.(A) SC data has been scaled logarithmically for visualization purpose. The rest (B & C) are presented in linear scale. The color bar represents the distribution of connectome values of the atlas.

side comparison of the measured SC, FC and predicted FC all in a same colorbar. From the Figure 2.4 we can already explore that there seems to be similar symmetric patterns emerging in the predicted FC. Later, we report the overall performance for the entire dataset wherein for each datapoint the result was reported for the model which did not use the respective datapoint while training. We first discuss some of the traditional performance metrics for regression problems as below.

2.7.3 MSE Map, Correlation Coefficient Map and Normalized Mutual Information Map

(i) The Correlation Coefficient Map or Corr-Coeff Map captures the Pearson product moment correlation between measured and predicted matrix's individual connectomes, (ii) The MSE map calculates the mean squared error between measured and predicted matrix's individual connectome across all data set. (iii) Mutual information is a quantity that measures a relationship between two random variables that are sampled simultaneously. Particularly, it measures how much information is contained, on average, in one random variable about another random variable. Normalized Mutual Information (NMI) is a measure used to evaluate the comprehensive findings of mutual information between two different partitions of dataset. The normalization simply ensures that NMI is 0 when there is no MI between two variables while NMI would

be 1 in the case of maximal MI (Lancichinetti et al., 2009). These three matrix maps provide the prediction performance at the level of individual connectomes. The higher the value of the correlation and normalized mutual information between the individual connectome of measured and predicted connectivity, the more the agreement between the measured/true and predicted values. In the case of MSE maps; lower values imply better agreement. By inspecting different parts of the matrices corresponding to the correlation coefficient, MSE or NMI map, we can analyze which connectomes or regions correspond to better performance as compared to other regions for a specific neural network structure. From the Figure 2.5 we can observe some of the characteristics of the individual connectome based on the correlation coefficient, MSE and NMI. For visualization purpose, the MSE map and the NMI map are logarithmically scaled. Our results show that the MSE map consists of lower values for majority of the regions. In the case of correlation coefficient, the values are evenly distributed across the spectrum. For the case of NMI, the pattern is inconclusive even after the log transformation.

2.7.4 Inverse Cumulative Histogram of the MSE, Corr-Coeff and NMI Map

The individual MSE, NMI and Corr- Coeff maps provide a visualization of the performance over individual connectome regions. However, it is still difficult to assess the overall performance for each testing fold and over all the individuals connectome values (in total N×N; in our case, N=360). We therefore propose to compute the inverse cumulative histograms (ICH) for the respective distributions of the MSI, NMI and Corr-Coeff maps for each of the five test folds. The ICH plots (from Figure 2.5) show for what percentage of connectome the model performance is bounded by what error. For the five folded cross validation, the value of the correlation starts from the range of (-0.8) to (-0.6) and then converges around (0.2); suggesting that the performance is consistent across all folds. The plots for MSE based map and NMI based map show similar distribution across folds

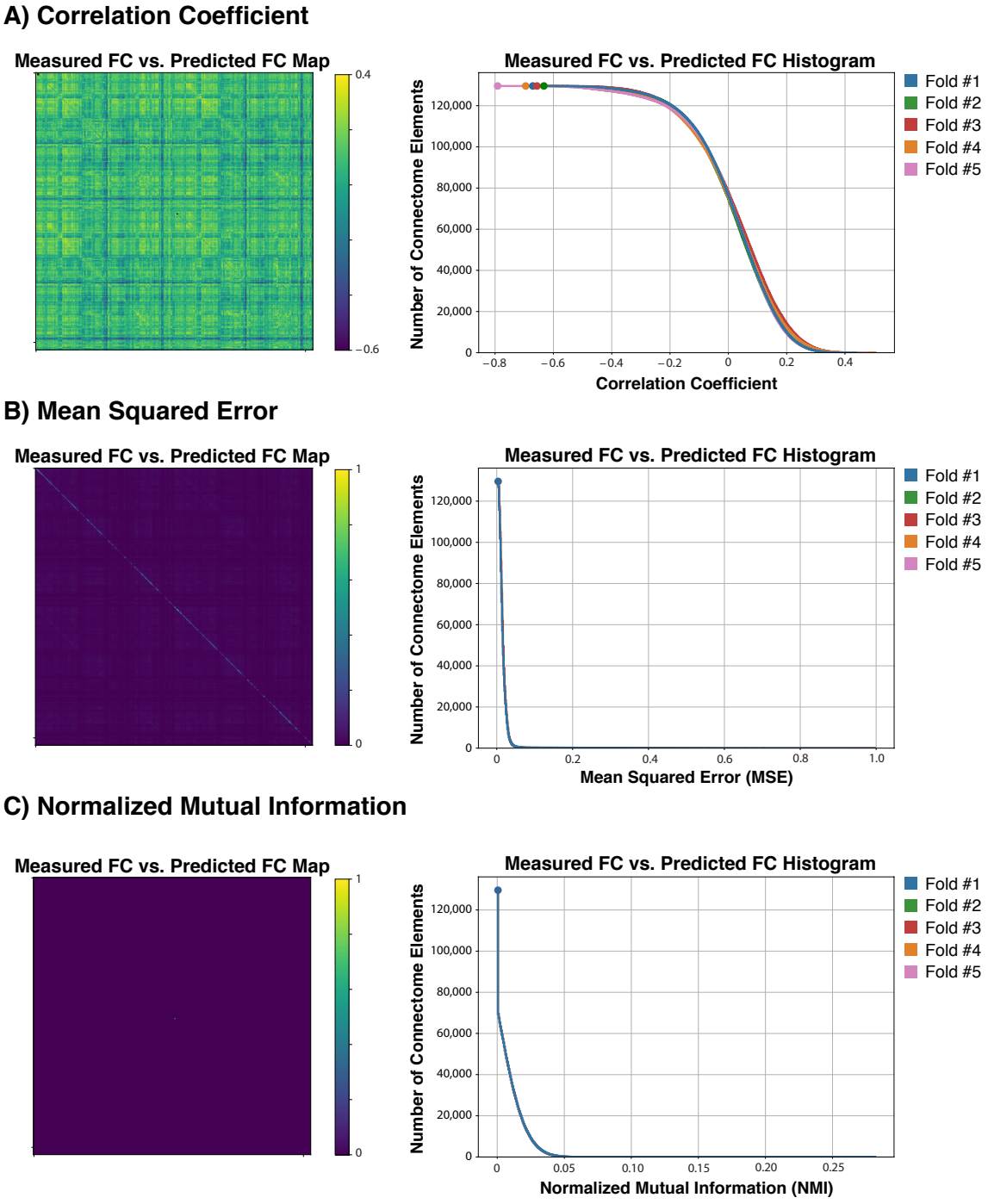

Figure 2.5: Correlation Coefficient (A) Mean Squared Error (B) and Normalized Mutual Information (C) between each regions of Measured Functional Connectivity and Predicted Functional Connectivity across all test data named as map (left hand side of the figure). The distribution of each participants folds is separately represented using a inverse cumulative histograms (right hand side of the figure).

2.7.5 Box and Whisker Plot

To evaluate the FC prediction performance effectively on the whole connectome for each participant, we vectorize the measured FC and the predicted FC and find out the Correlation Coefficients (Corr) and Normalized Mutual Information (NMI) and visualized the distribution of metrics using the box and whisker plot. We also compared it with the SC vs measured FC box plot. These box plots show that for each of the validations, the correlation between the measured FC and predicted FC is high (with some minor outliers). Despite the low correlation between the SC and the measured FC, the neural network was able to predict a highly correlated FC across all folds and on the whole dataset.

The two sets of boxplots (Figure 2.6) almost depict similar picture for each of the five folds. From Figure 2.6 we can observe that the correlation between the SC and measured FC is low and same goes for NMI as well. This trend remains consistent across all five folds. The high correlation between predicted and measured FC matrices, despite the low correlation between measured FC and SC, shows that the neural network was able to learn non-linear transformations between the input (SC) and the desired output (measured FC).

2.7.6 Connectome Fingerprinting Analysis

Human neuroimaging studies have reported some commonality of brain activity patterns across people. Despite this similarity, researchers have pointed out the differences in neurologically healthy brain structures and functions across population for specific tasks (Barch et al., 2013; Grabner et al., 2007; Newman et al., 2003; Rypma & D'Esposito, 1999). This principle can provide a distinct performance parameter for connectome-based outcomes. Researchers have (Finn et al., 2015) demonstrated that individual connectome profile can act as a unique identity for each person. Here we propose to co-opt this principle for the task of quantifying the performance of a regression model that attempts to predict FC. To designate traditional fingerprinting as a performance metric we evaluated the classification performance of identifying

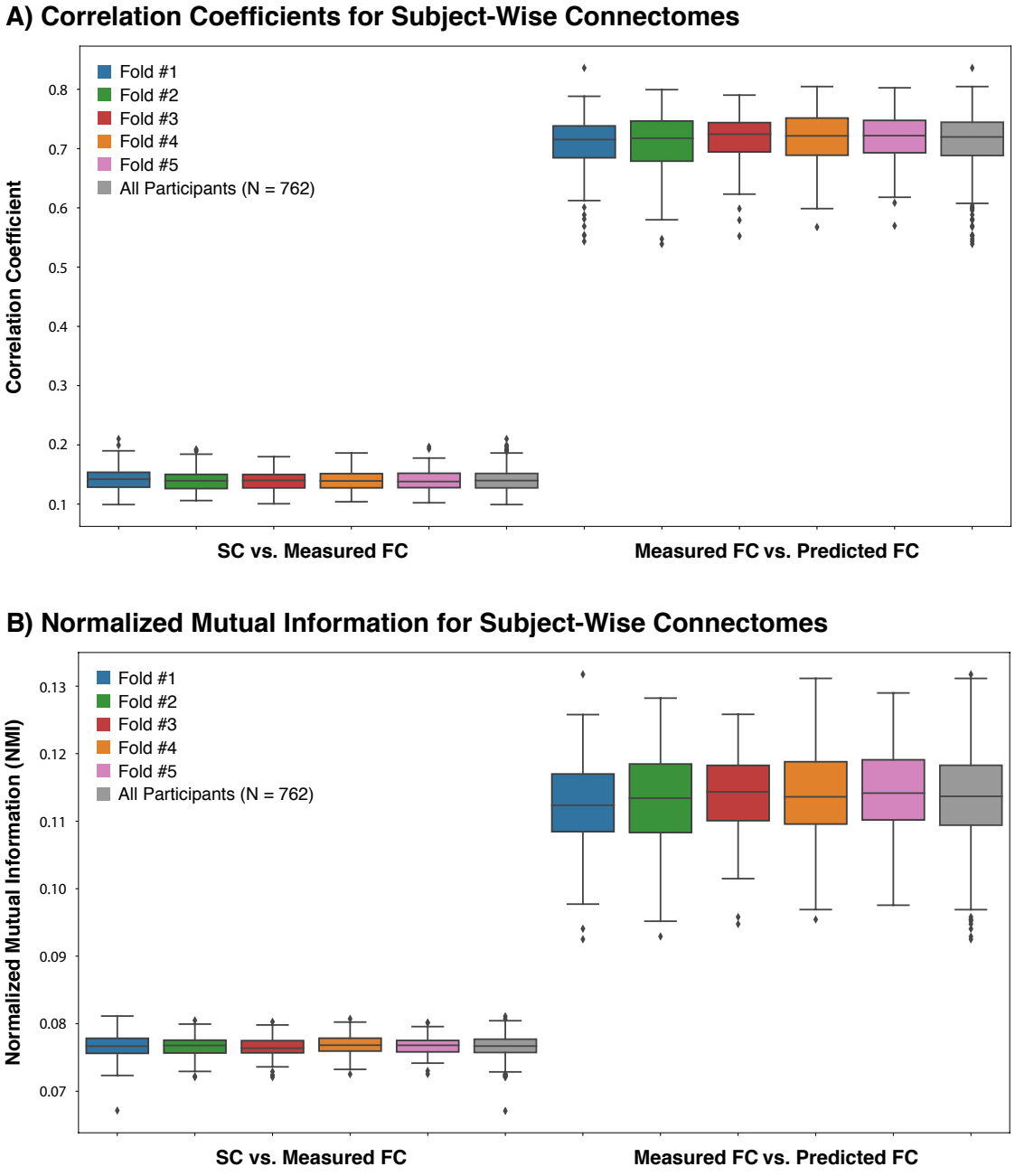

Figure 2.6: Low (but non zero) correlation between SC and FC, high correlation between measured vs predicted FC calculated via (A) Correlation Coefficients and (B) Normalized Mutual Information, and there are no difference between any of the 'folds'.

an individual based on predicted FC. In particular, if the predicted FC was closest (depending on MSE, NMI or Corr) to the measured FC of the same person, the individual classification was deemed correct. Traditional fingerprinting based performance is described in the Table 2.1.

Judging by the performance we can already observe that traditional fingerprinting is

Table 2.1: Estimated vs. Measured FC accuracy based on the traditional Functional Connectome Fingerprinting approach.

Data Used	**MSE-Based Accuracy(%)**	**Correlation-Based Accuracy(%)**	**NMI-Based Accuracy(%)**
GCN fold 1	3.28	6.57	5.26
GCN fold 2	3.28	11.84	5.92
GCN fold 3	7.23	7.23	6.57
GCN fold 4	3.94	5.92	7.23
GCN fold 5	5.84	9.74	7.14
GCN all participant	1.70	3.01	2.62

not effective in distinguishing each individual predicted from the AI-based algorithm. There are several reasons behind this anomaly: randomly distributed data, local maxima or minima in the comparison. In any cases, this is too hard for the FCF to find out the appropriate results for finding out the accuracy of the algorithm. To overcome these issues, we introduce the notion of Pairwise Functional Connectome Fingerprinting (PFCF), which can be an effective metric to quantify the overall performance of a regressor model trained to predict FC.

As discussed before, the principle behind PFCF is similar in spirit to the conventional functional connectome fingerprinting or FCF (Finn et al., 2015). However, rather than determine whether each predicted FC was closest to the measured FC of the respective individual, we estimated the probability that on average the model's predicted FC would be closest to measured FC of the corresponding person. Specifically, to compute PFCF for a given individual, the predicted FC is compared to the measured FC of the respective individual, and to the measured FC of other individuals one by one. If the predicted FC is closer to the correct measured FC, a counter is incremented. If there are N individuals in total, this would lead to $(N-1)$ comparisons. By keeping track of the count as to how many time over $(N-1)$ comparisons, the predicted FC turns out to be closer to the measured FC of the said individual, we can thus assign an estimated probability of fingerprinting done pairwise. In each pairwise

comparison, we made the decision in turn of the following metrics: correlation coefficient, normalized mutual information, and mean squared error. Later we took the average across the total number of tests to find out the PFCF for the algorithm.

From the chart 2.7(A) we can observe that we have a mean MSE based accuracy of 55.52%, Correlation Coefficient based accuracy of 64.01% and mean NMI based accuracy of 59.95% when calculated across five folds. In general terms, based on the predicted result, GCN based network was able to correctly identify 64% time among the other test participants when comparing between each possible configuration of the pairing. For all participants, among N_{Trials} = 762 (the number of participant) × 761 (the number of comparison between one to other participants) = 579,882 trials, PFCF performed as expected, and its Cumulative Distribution Function (CDF) obeys a binomial distribution. In particular, in Figure 2.7(B), the Binomial distribution curve shows the probability of getting a specific PFCF by chance. The graph also shows that to be statistically significant, having an accuracy of 50.11% would suffice but all three of our accuracies are much more than that. Figure 2.7 (C, D, E) specifies how the accuracy histogram varied along sorted participant numbers. And since its plotted using the mean accuracy, the area under the accuracy histogram represents the mean accuracy. The Participants Greater Than Chance (PGTC) accuracy specifies the accuracy if we considered the accuracy greater than 50% for all the people. In all cases, the result is statistically significant as observed from the p-value.

2.8 Discussion

The overarching goal of the current project was to promote transparency, repeatability, and direct comparisons between future AI-based human brain SC-FC mapping studies. Therefore, in addition to describing, sharing, and characterizing a large, open-access dataset (consisting of subject-specific SC, sFC, dFC_Max, dFC_Min, and dFC_Var connectomes), we have also proposed a minimal set of performance evaluation parameters that can be used to benchmark different AI-based SC-FC (or FC-SC) predictions. In this paper, we introduced a novel benchmarking parameter for evalu-

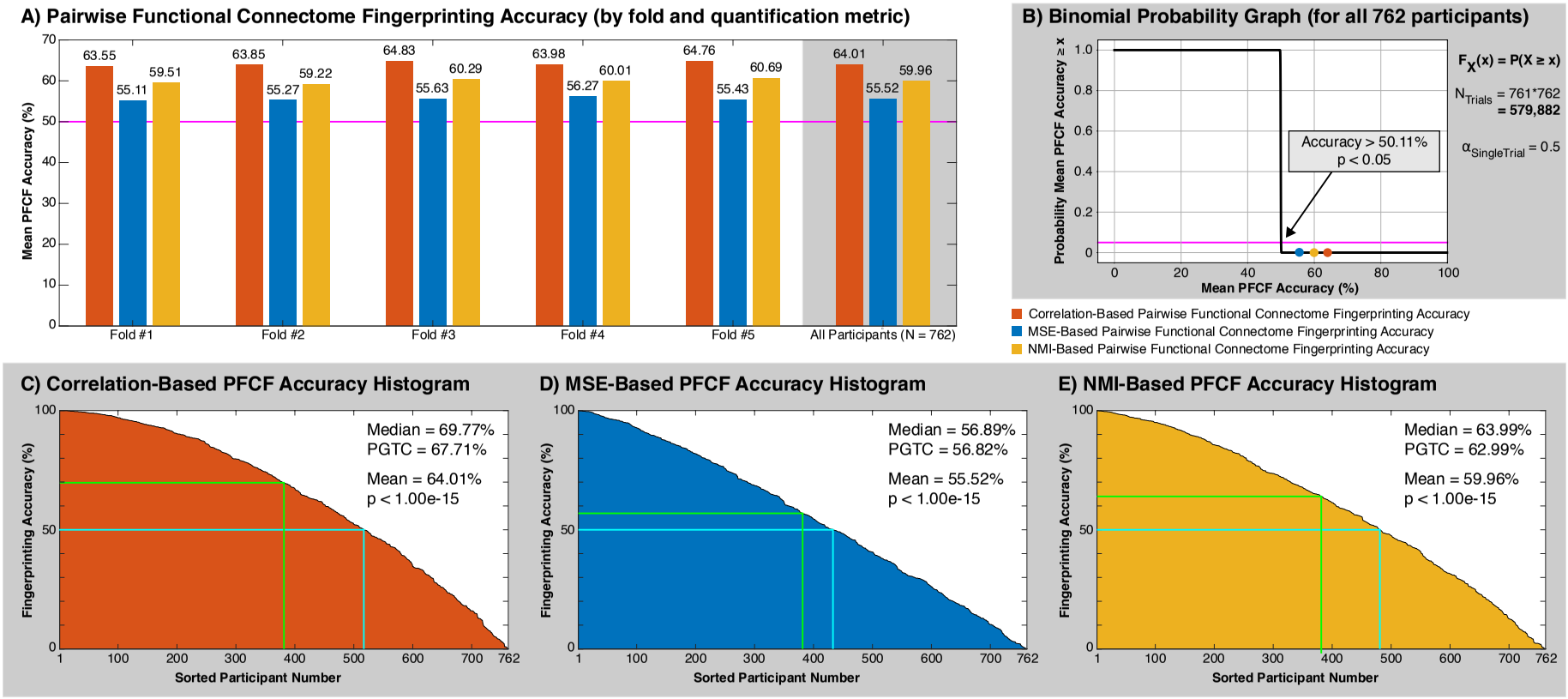

Figure 2.7: (A) PFCF accuracy across all folds & for all participants altogether where we can observe similar trends for each different scenario, (B) Binomial Probability Graph for all 761 trials on each 762 participants; the shape of the graph reveals that there is less than a 5% probability of getting an accuracy $> 50.11\%$ which are random, (C), (D), (E) specifies how the accuracy convolves around the participant number through histogram calculated via Correlation Coefficient, MSE & NMI. In each case, getting a mean accuracy is highly significant as we can observe from the range of p value ($p < 1.00e\text{-}15$). The Participants Greater than Chance (PGTC) & the Median accuracy can be accumulated from the histograms to evaluate the overall result of the fingerprinting performance.

ating the performance for machine learning based brain connectivity analysis. Using a graph- based Convolutional neural network, we predicted the FC from the SC. For evaluating the performance of the prediction, we suggest that each of the parameters of the evaluation demonstrates different set of objectives of the performance evaluation. We propose that the combination of this parameters can evaluate the performance of individual algorithms as well as how well they are performing on specific connectomes. Considering the progress of recent artificial intelligence-based methods, we anticipate more research along the lines of deep learning for predicting brain connectivity analysis in the imminent future. As such, the proposed performance metrics in this work can be used to benchmark the future AI based algorithms in a standardized way.

2.9 Acknowledgement

The project was supported by NSERC Discovery Grant, Thorlakson Foundation Grant, and the Compute Canada Research Computing Cluster. The preprocessed and segmented SC edge-weight and FC time-course HCP data used in this paper were kindly provided by Dr. Petra Ritter (Charite–Universittsmedizin Berlin).

References

Allen, E. A., Damaraju, E., Plis, S. M., Erhardt, E. B., Eichele, T., & Calhoun, V. D. (2014). Tracking whole-brain connectivity dynamics in the resting state. *Cerebral cortex*, *24*(3), 663–676.

Barch, D. M., Burgess, G. C., Harms, M. P., Petersen, S. E., Schlaggar, B. L., Corbetta, M., Glasser, M. F., Curtiss, S., Dixit, S., Feldt, C., et al. (2013). Function in the human connectome: Task-fmri and individual differences in behavior. *Neuroimage*, *80*, 169–189.

Bullmore, E., & Sporns, O. (2009). Complex brain networks: Graph theoretical analysis of structural and functional systems. *Nature reviews neuroscience*, *10*(3), 186–198.

Bullmore, E., & Sporns, O. (2012). The economy of brain network organization. *Nature reviews neuroscience*, *13*(5), 336–349.

Finn, E. S., Shen, X., Scheinost, D., Rosenberg, M. D., Huang, J., Chun, M. M., Papademetris, X., & Constable, R. T. (2015). Functional connectome fingerprinting: Identifying individuals using patterns of brain connectivity. *Nature neuroscience*, *18*(11), 1664–1671.

Glasser, M. F., Coalson, T. S., Robinson, E. C., Hacker, C. D., Harwell, J., Yacoub, E., Ugurbil, K., Andersson, J., Beckmann, C. F., Jenkinson, M., et al. (2016). A multi-modal parcellation of human cerebral cortex. *Nature*, *536*(7615), 171–178.

Grabner, R. H., Ansari, D., Reishofer, G., Stern, E., Ebner, F., & Neuper, C. (2007). Individual differences in mathematical competence predict parietal brain activation during mental calculation. *Neuroimage*, *38*(2), 346–356.

Honey, C. J., Kötter, R., Breakspear, M., & Sporns, O. (2007). Network structure of cerebral cortex shapes functional connectivity on multiple time scales. *Proceedings of the National Academy of Sciences*, *104*(24), 10240–10245.

Honey, C. J., Sporns, O., Cammoun, L., Gigandet, X., Thiran, J.-P., Meuli, R., & Hagmann, P. (2009). Predicting human resting-state functional connectivity from structural connectivity. *Proceedings of the National Academy of Sciences*, *106*(6), 2035–2040.

Hutchison, R. M., Womelsdorf, T., Allen, E. A., Bandettini, P. A., Calhoun, V. D., Corbetta, M., Della Penna, S., Duyn, J. H., Glover, G. H., Gonzalez-Castillo, J., et al. (2013). Dynamic functional connectivity: Promise, issues, and interpretations. *Neuroimage*, *80*, 360–378.

Kim, M., Bao, J., Liu, K., Park, B.-y., Park, H., & Shen, L. (2020). Structural connectivity enriched functional brain network using simplex regression with graphnet. *International Workshop on Machine Learning in Medical Imaging*, 292–302.

Kingma, D., & Ba, J. (2015). Adam: A method for stochastic optimization3rd international conference on learning representations, iclr 2015. *International Conference on Learning Representations, ICLR*.

Kipf, T. N., & Welling, M. (2016). Semi-supervised classification with graph convolutional networks. *arXiv preprint arXiv:1609.02907*.

Lancichinetti, A., Fortunato, S., & Kertész, J. (2009). Detecting the overlapping and hierarchical community structure in complex networks. *New journal of physics*, *11*(3), 033015.

Leonardi, N., & Van De Ville, D. (2015). On spurious and real fluctuations of dynamic functional connectivity during rest. *Neuroimage*, *104*, 430–436.

Li, Y., Shafipour, R., Mateos, G., & Zhang, Z. (2019). Mapping brain structural connectivities to functional networks via graph encoder-decoder with interpretable latent embeddings. *2019 IEEE Global Conference on Signal and Information Processing (GlobalSIP)*, 1–5.

Mišić, B., Betzel, R. F., De Reus, M. A., Van Den Heuvel, M. P., Berman, M. G., McIntosh, A. R., & Sporns, O. (2016). Network-level structure-function relationships in human neocortex. *Cerebral Cortex*, *26*(7), 3285–3296.

Neudorf, J., Kress, S., & Borowsky, R. (2022). Structure can predict function in the human brain: A graph neural network deep learning model of functional connectivity and centrality based on structural connectivity. *Brain Structure and Function*, *227*(1), 331–343.

Newman, S. D., Carpenter, P. A., Varma, S., & Just, M. A. (2003). Frontal and parietal participation in problem solving in the tower of london: Fmri and computational modeling of planning and high-level perception. *Neuropsychologia*, *41*(12), 1668–1682.

Park, H.-J., & Friston, K. (2013). Structural and functional brain networks: From connections to cognition. *Science*, *342*(6158), 1238411.

Paszke, A., Gross, S., Massa, F., Lerer, A., Bradbury, J., Chanan, G., Killeen, T., Lin, Z., Gimelshein, N., Antiga, L., Desmaison, A., Kopf, A., Yang, E., DeVito, Z., Raison, M., Tejani, A., Chilamkurthy, S., Steiner, B., Fang, L., ... Chintala, S. (2019). Pytorch: An imperative style, high-performance deep learning library. In H. Wallach, H. Larochelle, A. Beygelzimer, F. d'Alché-Buc, E. Fox, & R. Garnett (Eds.), *Advances in neural information processing systems 32* (pp. 8024–8035). Curran Associates, Inc. http://papers.neurips.cc/paper/9015-pytorch-an-imperative-style-high-performance-deep-learning-library.pdf

Rypma, B., & D'Esposito, M. (1999). The roles of prefrontal brain regions in components of working memory: Effects of memory load and individual differences. *Proceedings of the National Academy of Sciences*, *96*(11), 6558–6563.

Sarwar, T., Tian, Y., Yeo, B. T., Ramamohanarao, K., & Zalesky, A. (2021). Structure-function coupling in the human connectome: A machine learning approach. *NeuroImage*, *226*, 117609.

Savva, A. D., Mitsis, G. D., & Matsopoulos, G. K. (2019). Assessment of dynamic functional connectivity in resting-state fmri using the sliding window technique. *Brain and behavior*, *9*(4), e01255.

Shannon, C. E. (1949). *The mathematical theory of communication, by ce shannon (and recent contributions to the mathematical theory of communication), w. weaver*. University of illinois Press Champaign, IL, USA.

Smith, S. M., Beckmann, C. F., Andersson, J., Auerbach, E. J., Bijsterbosch, J., Douaud, G., Duff, E., Feinberg, D. A., Griffanti, L., Harms, M. P., et al. (2013). Resting-state fmri in the human connectome project. *Neuroimage*, *80*, 144–168.

Sotiropoulos, S. N., Jbabdi, S., Xu, J., Andersson, J. L., Moeller, S., Auerbach, E. J., Glasser, M. F., Hernandez, M., Sapiro, G., Jenkinson, M., et al. (2013). Advances in diffusion mri acquisition and processing in the human connectome project. *Neuroimage*, *80*, 125–143.

Sporns, O. (2007). Brain connectivity. *Scholarpedia*, *2*(10), 4695.

Strehl, A., & Ghosh, J. (2002). Cluster ensembles—a knowledge reuse framework for combining multiple partitions. *Journal of machine learning research*, *3*(Dec), 583–617.

Tournier, J.-D., Calamante, F., & Connelly, A. (2012). Mrtrix: Diffusion tractography in crossing fiber regions. *International journal of imaging systems and technology*, *22*(1), 53–66.

Van, R. G., & Drake, F. (2009). Python 3 reference manual. *Scotts Valley, CA: CreateSpace*, *10*, 1593511.

Van Den Heuvel, M. P., & Pol, H. E. H. (2010). Exploring the brain network: A review on resting-state fmri functional connectivity. *European neuropsychopharmacology*, *20*(8), 519–534.

Van Essen, D. C., Smith, S. M., Barch, D. M., Behrens, T. E., Yacoub, E., Ugurbil, K., Consortium, W.-M. H., et al. (2013). The wu-minn human connectome project: An overview. *Neuroimage*, *80*, 62–79.

Zhang, L., Wang, L., & Zhu, D. (2020). Recovering brain structural connectivity from functional connectivity via multi-gcn based generative adversarial network. *International Conference on Medical Image Computing and Computer-Assisted Intervention*, 53–61.

Zimmermann, J., Griffiths, J., Schirner, M., Ritter, P., & McIntosh, A. R. (2018). Subject specificity of the correlation between large-scale structural and functional connectivity. *Network Neuroscience*, *3*(1), 90–106.

Chapter 3

Comparison of deep learning architectures for subject specific structural to functional brain connectivity mapping

3.1 Abstract

Earlier studies have found out that resting state functional connectivity can be predicted from structural connectivity through computational modelling and artificial intelligence (AI) based methods. Computational modelling as well as AI-methods have been used to analyze these connectivity-based parameters. However, due to the complexity involved in predicting each individual connectivity, traditional comparison methods do not capture the true performance of the algorithm. Using the recent AI-based connectivity evaluation parameter such as Pairwise Functional Connectome Fingerprinting and other predefined evaluation parameters, this study aims to analyze the baseline performance and methods to improve the performance using different architectural designs based off the templates of U-Net and Graph Convolutional Network.

3.2 Introduction

The human brain is an amazing organ. Despite having a static structure, it controls quite a lot of intrinsic functions and cognitive purposes. The significance of this performance may lie within the brain's innate network architecture. In recent times, with

the invention of non-invasive neuroimaging techniques, researchers can measure the intrinsic inter regional connectivity (Gui et al., 2010). The human brain connectivity refers to the inter-regional connections (structural connectivity or SC) or statistical dependencies (functional connectivity or FC) (Sporns, 2007). Initial studies (Honey et al., 2007; Honey et al., 2009) have revealed some insight about the underlying relationship between structural and functional connectivity. After the initial proof of concepts, several other studies have demonstrated using computational modelling (Greicius et al., 2009; Mišić et al., 2016) as well as artificial intelligence-based methods (Kim et al., 2020; Y. Li et al., 2019; Lin et al., 2021; Zhang et al., 2020) to map the brain's SC to FC. As discussed in the previous chapter, this prediction can be configured as a regression-based task from the machine learning viewpoint. Due to the brain's complexities involved around connectome analysis, traditional regression-based methods performs poorly in predicting one form to another. From our earlier findings we explored how traditional regression-based performance indicators do not completely capture and quantify the performance of different algorithms, proposed a set of standardized benchmarking parameters for AI-based SC-FC predictions, and then provided an initial proof-of-principle using a single implementation of a Graph Convolutional Network (GCN). As a next step towards improving the performance, in this paper, we propose to use two different types of deep neural algorithm architectures, U – Net (Ronneberger et al., 2015) and GCN (Kipf & Welling, 2016), while also varying different parameters for each, to predict functional connectivity from structural connectivity. Along with other performance comparison parameters, we propose to use the Pairwise Functional Connectome Fingerprinting (PFCF) approach based on the traditional fingerprinting (Finn et al., 2015) to compare the performance evaluation of the algorithms. Using these performance parameters, we have modified the architecture to evaluate the improvement of the performance.

3.3 Methods & Materials

This section describes in detail about the general implementation and various modifications made to each type of algorithm as well as the basic preprocessing of the data.

3.3.1 Description of the Data

We obtained the neuroimaging (dwMRI and rs-fMRI BOLD) data from HCP (Van Essen et al., 2013) (S900 release) for 762 subjects. The Glasser atlas (Glasser et al., 2016) was used for defining the Regions of Interest (ROI) for calculating SC and FC. Each subject's SC matrix was constructed via quantifying connected edges (of the 360 Glasser atlas ROI pairs using the weighted streamline count (SIFT2) by cross-sectional area method (Smith et al., 2013)) between the pair of ROIs of the atlas. The FC data were included with four separate scans, each consisting of 1200 time points and having been segmented using the same 360 ROI Glasser atlas. Finally, the static FC matrix was calculated as the bivariate correlation between the BOLD time series within each pair of ROIs. The detailed procedure of the data processing is available in the previous chapter 2. For the context of our study, we will only be focusing on the static FC prediction from the SC.

3.3.2 Graph CNN and Its Modifications

In a traditional CNN, the neighbourhood of interacting pixels depends on the filter size, and it does not justify the inbuilt structure of the brain connectivity matrix. The main motivation for implementing graph-based structures, is to compensate the complex relationship between data and the modelling parameters associated with the brain connectivity. Both the structural and functional connectivity matrices can be represented into graph structures, where different ROI's can act as the nodes and the connection strength between each of the nodes acts as the edge weight of the graph. Our implementation of the GCN was subdivided into three basic structures with some architectural variations in the last layer. Details of the architectural variations are

described in the following sections.

Following the initial proof of concept regarding SC-FC prediction (from Chapter 2), we started our analysis on the Graph CNN from (Y. Li et al., 2019) with some different architectural modifications. In previous experiments, we observed that the network needed more learnable parameters to map the complexities , and the nature of the decoder in our original GCN - specifically the use of tanh(ReLU) - only allowed for the prediction of positive FC values.. We focused more on introducing these parameters and modifying the implementation to allow the network to learn both positive and negative FC values.

The main architecture of the GCN can be partitioned into three main parts; the preprocessing, the encoder, and the decoder; each having their own operation. In the preprocessing step, we make the data compatible for the encoder network. Consider an undirected graph denoted by $G = (V, A_{\mathrm{ij}})$, where V is the set of the nodes of the connected brain regions and $\mathrm{A_{i,j}}$ represents the connection strength between regions i and j of the symmetric connectivity. For the preprocessing we make $\mathrm{A_{ij}}$ mapped into adjacency matrix $\hat{A}$ where

$$\widehat{A} := \tilde{D}^{\frac{-1}{2}} \tilde{A} \tilde{D}^{\frac{-1}{2}}$$

$\tilde{D}$ is the degree matrix of the input $\tilde{A}$, where $\tilde{A} = I + A_{\mathrm{i,j}}$,where I is the identity matrix of the input A.

For the encoder part, a single layer Graph CNN can be constructed as

$$E_1 = ReLU(\widehat{A} X \theta)$$

where, ReLU stands for Rectified Linier Unit and can be written as ReLU(P) = max(0,P). X stands for the nodal attributes of the graph. The nodal attributes can consist of any number of features; however, for all the consequent models in this study we have used a one-hot representation for each node only to have the notion of each node being identifiable distinctly. That is why we chose $X \epsilon \mathbb{R}^{N \times K}$, where N is the number of nodes in the brain region (in our case its N=360), K is the node ID's (in our case, K = 360). The weight parameter θ is being updated with the convolution

layer filter coefficients. It is defined as $\theta \epsilon \mathbb{R}^{K \times F}$; where F is number of filters in the convolution layer (since we are using a 360 based connectome, we started with F=360 and then concatenated F = 300, 250). From the initial baseline study, it was intuitive to add more layers to enable the architecture to learn more configurations of the functional connectivity, and also allow more parameters to permit the model to learn more complexities about the data. That is why we experimented with different configurations of θ. In this paper, there were three combinations of encoder layers (total six configurations; details are described in the later parts of the paper), cascaded one after another to map out the complex relationship of FC from SC. A batch normalization is used for normalizing the values before going to the next layer. The configuration of K and F are based on our choice and for this experiment we started with different permutation and combination but finally reported these three combinations for parameter F. The encoder can be implemented as a cascading layer configuration, so for the case of the consequent encoder E_1, E_2 or E_3 , the output of one layer goes to the input of the next layer after a non-linear activation.

To approximate the FC matrix via the adjacency matrix and nodal attributes, the output of the single layer/multi-layer encoder goes to the decoder, which can be defined as

$$Z = tanh(ReLU(EE^T))$$

where $tanh(x) = \frac{e^x - e^{-x}}{e^x + e^{-x}}$. E is the output of the final encoder layer. In our test case scenario, we observed the range of values of FC is from -1 to 1, although the values are more skewed towards positive correlations. To map these values at the appropriate range, we opted to use tanh activation alone (allowing the algorithm to learn only positive FC values), as well as a combination of tanh and ReLU activation (only one activation function such as tanh will allow the algorithm to learn both positive and negative range of values). Since the experimentation of (Y. Li et al., 2019) involved adding an extra ReLU activation layer, their GCN implementation experiments only allowed the prediction of positive parts of the FC. But in our case, we implemented both variations to allow the neural network to gain more flexibility in the predicted

values. Figure 3.1 (A) shows all the configurations of the GCN along with its selections of non-linearity for both configurations.

3.3.3 U-Net and Its Modifications

U-net's name is inspired from its architectural configuration (Ronneberger et al., 2015). The layout consists of a contraction block followed by an expansion block , with each block consisting of several sub block operations such as convolution, pooling and activation layers. The advantage of such a structure is that it retains the structural context along the contraction path without the loss of any semantic details (Ronneberger et al., 2015). Although it was initially used as a solution for segmentation problems, this contraction and expansion of the configuration can be used in regression problems as well. We started with a simple configuration but added more complexities (layers and normalization techniques) for mapping out the features. Finally, our architecture consists of six stages along the contraction (two convolution layers, two ReLU's, two batch normalizations) and three stages on the expansion (one convolutions, one ReLU's and one batch normalization). After each contraction feature maps, we included a max pool layer to down-sample the values before going to another contraction layer. We embedded five contraction blocks and five expansion blocks in the U- Net configuration. However, this initial configuration was not providing good prediction and one of the speculated reasons was that the embedding on the previous layers and the later layers may be inconsistent. Since the algorithm is able to capture the earlier feature set, one of our ideas was to get access to those weights and features and that is why we included skip connection (a concatenative connection between contraction block and expansion block) (He et al., 2016; H. Li et al., 2018). We therefore formulated two different variations of the algorithm, one with the concatenated skip connection and one with the "vanilla" configuration of contraction and expansion block. Figure 3.1 (B) shows all the configurations of the U-Net along with its selections of skip connection. The structural configuration is almost the same for both configurations, apart from a skip connection from convolution block to the up sample block (as pointed by the

green arrow).

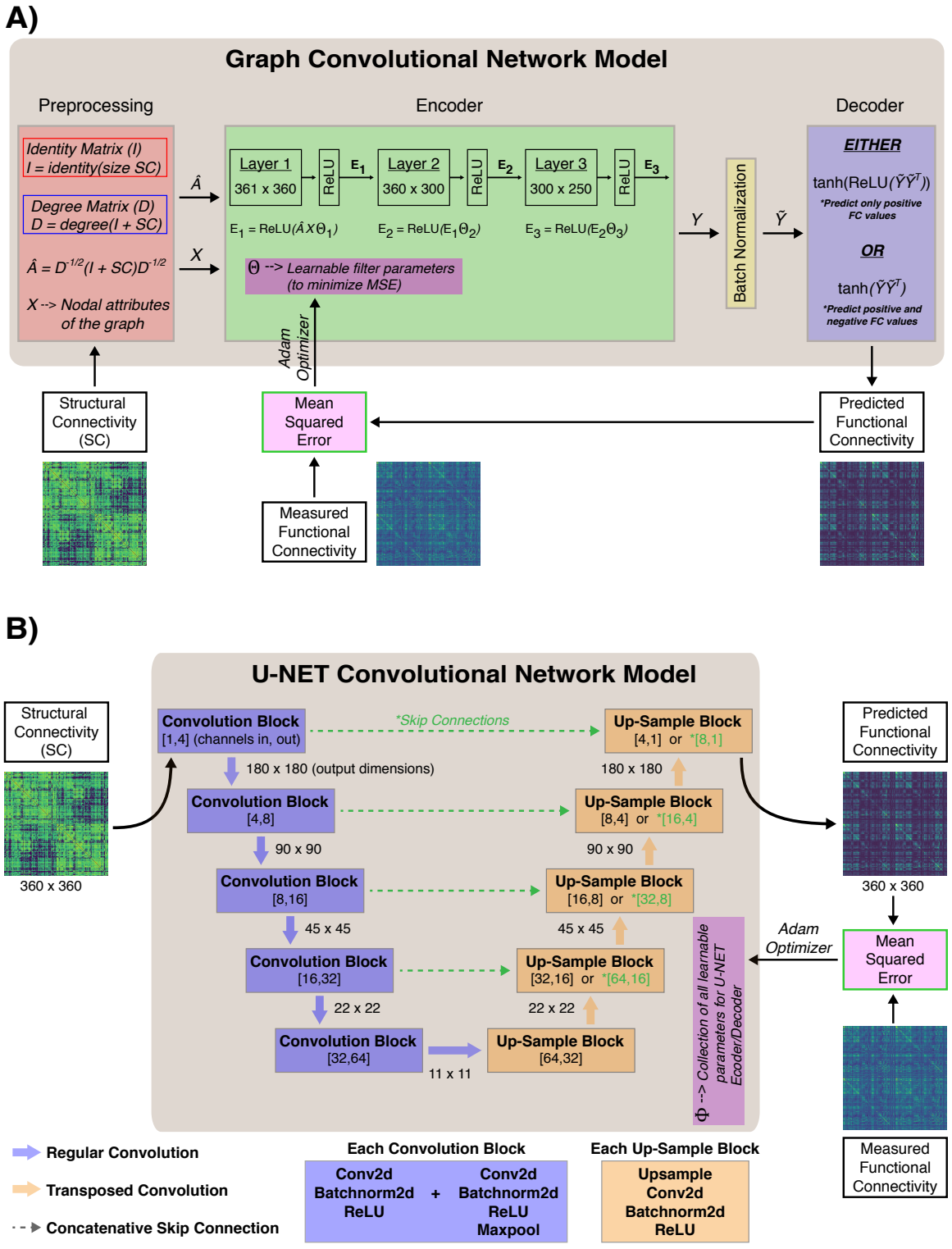

Figure 3.1: The experimented structures (A: GCN and all its variations, B: U-Net and its variations). The legend of the figure's specifies each type of structural differences and its architectural variations.

3.3.4 Experimental Setup

To train the model and adjust the weights and bias, mean squared error between the measured FC matrix and predicted FC matrix is selected as the loss function. Adam (Kingma & Ba, 2015) optimizer is used with a learning rate of 0.001 as the optimization algorithm. Each model is trained for 1000 epochs using a workstation equipped with quad Nvidia RTX-8000 GPUs. Both the U-Net and GCN were implemented in the PyTorch framework (Paszke et al., 2019). For our performance evaluations, all 762 subjects were randomly parcellated into 5-fold distribution (80% for training and 20% for testing the performance). To reduce the complexities, we only reported the results across all the participants (all folds together). In our experiment, we experimented with these following configurations.

GCN Based Analysis

- One-layer (360 layers), Node Id's as Nodal Embedding.
- Two-layer (360, 300), Node Id's as Nodal Embedding.
- Three-layers (360, 300, 250), Node Id's as Nodal Embedding.

U-Net Based Analysis

- U-Net with vanilla configuration
- U-Net with skip connection.

For naming each configuration, we used a numeric approach. Each of the GCN is subdivided into two configurations, the only structural difference is the added activation layer. So, the one-layer GCN (360 layers) is named as GCN#1 (with ReLU and tanh as the activation function) and GCN#2 (with tanh). Consequently, two layer GCN is similarly named as GCN#3 (with ReLU and tanh) and GCN#4 (with tanh) . In summary, the naming configuration of GCNs are as follows:

- GCN#1: One layer GCN (360 layer), ReLU and tanh as activation functions.
- GCN#2: One layer GCN (360 layer), ReLU as activation function.

- GCN#3: Two layer GCN (360 layer, 300 layer), ReLU and tanh as activation functions.
- GCN#4: Two layer GCN (360 layer, 300 layer), ReLU as activation function.
- GCN#5: Three layer GCN (360 layer, 300 layer, 250 layer), ReLU and tanh as activation functions.
- GCN#6: Three layer GCN (360 layer, 300 layer, 250 layer), ReLU as activation function.

The U-Net with the vanilla configuration and with the skip connection are named as U-NET#1 and U-NET#2. Figure 3.2 shows all the predicted FC for all architectural configuration in same colorbar. It is apparent from figure 3.2 that, the GCN architectures all performed better than either of the U-Net architectures.

3.4 Result Evaluation Parameters

Each participant's fold has been trained with the respective training fold using the above 8 configuration and predicted using the testing fold. For simplifying all the result parameters, after the test of each fold, it has been calculated for the whole population (all of 762 participants). All the result evaluation parameters that are presented here are based on the 762 participants compiled over the algorithms.

3.4.1 Correlation Maps and Inverse Cumulative Histogram

The idea behind using correlation map was to have an in-depth sense about how the individual connectomes performed on the prediction. Based on the atlas configuration, the individual connectomes are arranged. So, we wanted to explore how each unique connectomes are predicted using the algorithms through using the correlation map. The map captures the product moment correlation between measured and predicted matrix's individual connectomes. By observing the individual section of the correlation coefficient of MSE map, we can judge which connectomes or regions performs better than other regions for a specific neural network structure. The inverse cumulative

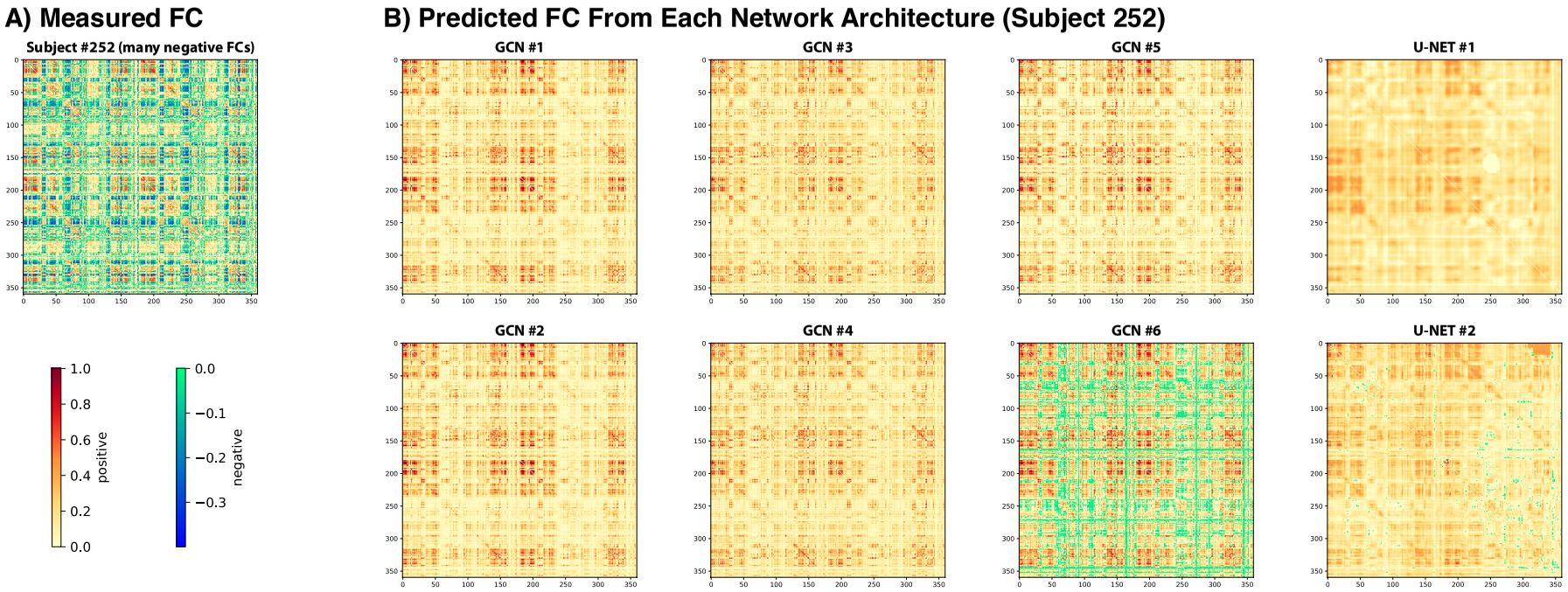

Figure 3.2: Measured Functional Connectivity and its predicted Functional Connectivity from different architectural combination (all the pictures are scaled in a same way). Note that, GCN performed better than U-Net (apparent from the visualization). In-depth analysis of the performance are described in the later figures and process of analysis.

histogram (ICH) draws the correlation map in a more expressive manner. Rather than showing all the connectomes in a communicative manner in a single picture, the inverse cumulative histogram demonstrates a distribution of correlation in a X-Y allocation. In an ideal case, with consistently higher correlation, the ICHs will become more skewed towards the right.

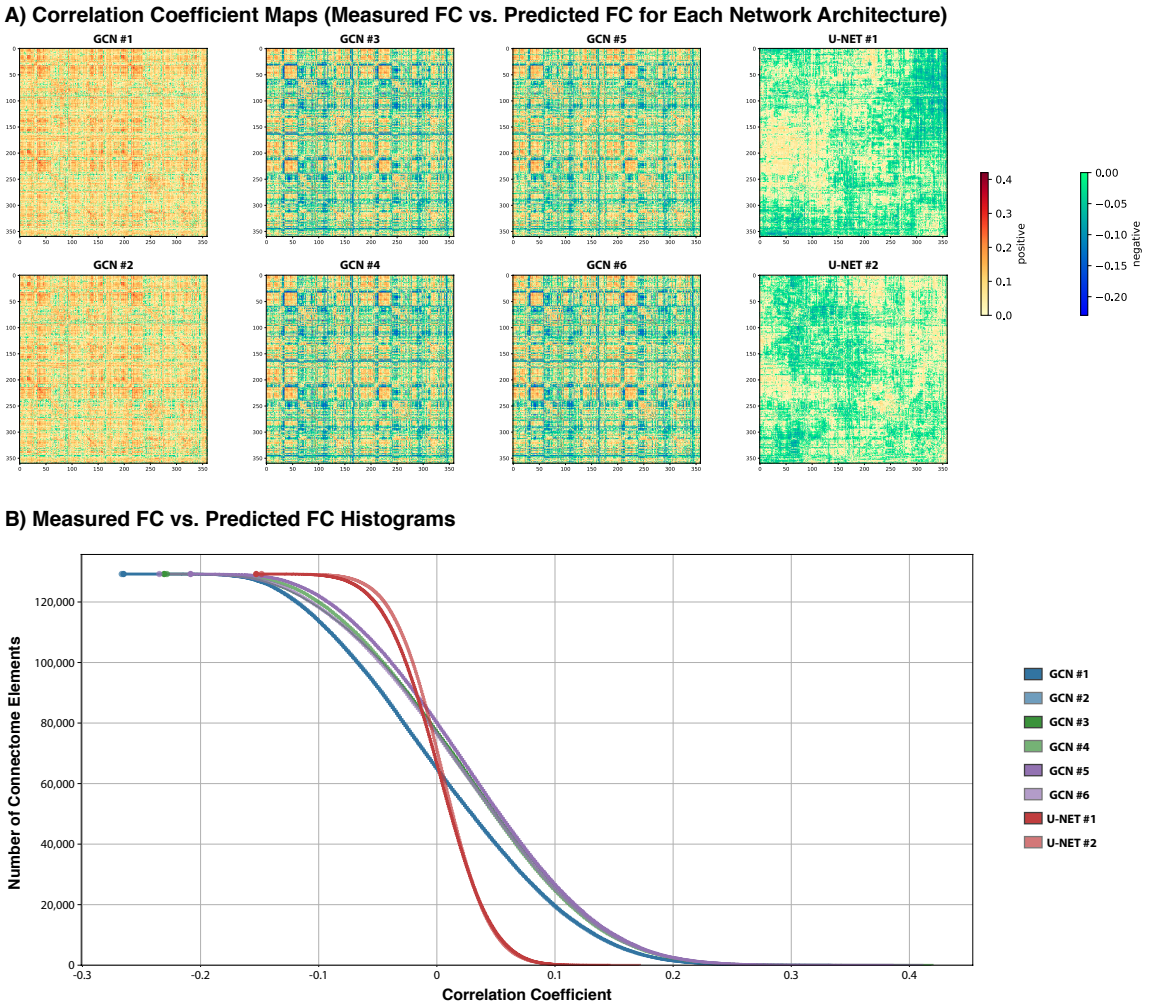

Figure 3.3: A) Correlation map specifies Correlation Coefficient across each individual connectome across the whole population. This connectome map specifies the performance of each individual connectome across the measured and predicted values. B) Captures the correlation coefficient in a more expressive manner where the result is expressed in a X-Y scatter plot.

In our case, from Figure 3.3, GCN#1 and GCN#2 have low resemblance with the measured FC values compared to the other GCN implementations. Since it does not have much complex layers, it can be assumed that it may not be "dense" enough to

learn all the complex configurations. We can get more idea about it in the inverse cumulative histograms. The values for the connectomes are skewed towards -0.3 which is also apparent from the correlation maps. GCN#3 to GCN#6 performed quite similarly and we can observe their values through their respective cumulative histograms. Although we allow the network to learn more negative values (hence adding two different activation layers), the number of predicted negative FC values was generally fairly small. The performance of U-Net was not as good as the GCN architectures, and we can see that maximum correlations lie between -0.1 and 0.1. The main idea behind these two parameters is to get a quick overall idea about the overall performance of an algorithm towards connectivity analysis and from that we can observe that GCN performed better than U-Net in almost every case despite predicting a combination of both positive and negative values.

3.4.2 Box and Whisker Plot

Using the correlation coefficient and mean squared error as the parameters for evaluation, we vectorized the measured functional connectivity and predicted functional connectivity across the entire group of 762 participants and visualized them using a box and whisker plot. The idea behind this visualization is to get an overall notion about how each of the algorithms is performing from the individual participant level. Through boxplot, we also get an estimate about the outliers (the upper and lower extremes) and values between interquartile range (IQR). In the ideal case, the correlation coefficients should be higher (larger correlation between the measured and predicted FC values) and the mean squared error should be lower (smaller difference between the measured and predicted FC values).

From the Figure 3.4, we can evaluate the performance of the deep learning based architectures. It is apparent from the boxplots that different variations were similar within each architecture (all six GCNs were similar to each other, and both U-Nets were somewhat similar to each other), . Among the six GCNs, the GCN#4 – GCN#6 performed almost similar. From the correlation coefficient boxplot, we can deduce that

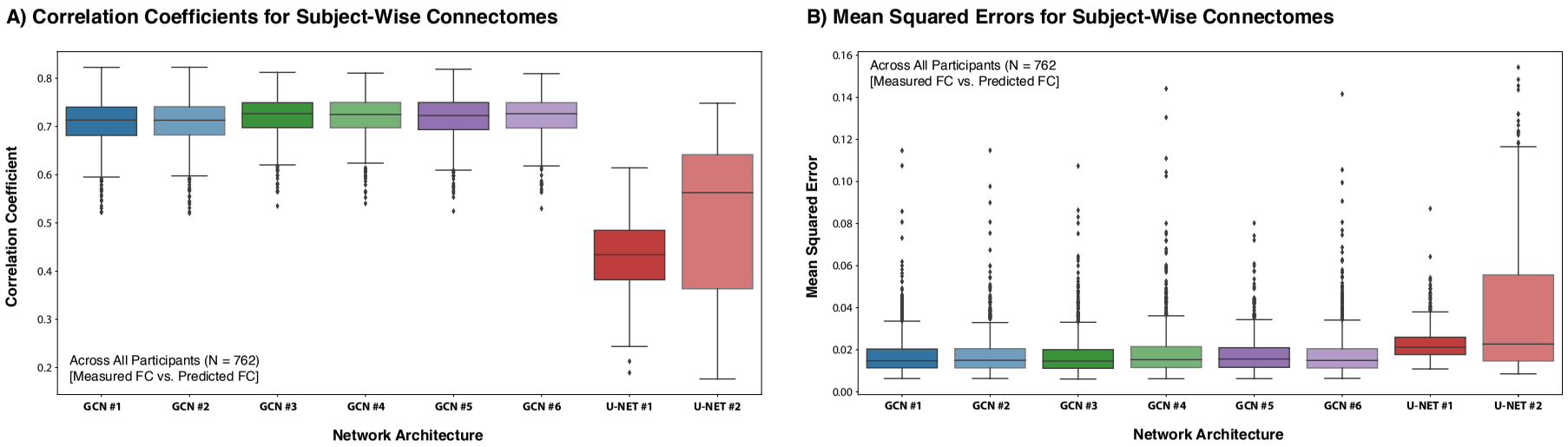

Figure 3.4: The box and whisker plot of eight configurations across all participants calculated via A) Correlation Coefficients B) Mean Squared Error. The performance indicator is about higher the correlation coefficient or lower the MSE, better the performance.

they have an upper range of 0.8 (in those cases the algorithms were able to reproduce the predicted connectomes significantly) and a lower extreme range of around 0.63. Their IQR width is almost similar, and median is around 0.72. The outliers lie mostly around on the lower end. For GCN#1 and GCN#2 the performance is almost analogous with the other GCN, with the most notable difference being the lower extreme range around 0.6. The U-Net#1 and #2 performed inferior to the GCNs. Both the U-Nets best performance was for 0.6 and 0.7 respectively. The IQR for U-Net#2 is far wider than the rest of the algorithms; stating that it contains a wide range of correlation from 0.4 to 0.6. The same story goes for the mean squared error based correlations. Here almost all the GCNs show a similar trend with a wide range of upper outlier from 0.04 – 0.14. The U-Net's performance was inferior to the GCN, and it shows a wide range of values from 0.01 - 0.06 with the outliers ranging in 0.16. So, from this we can deduct that GCN performed better than the traditional U-Net.

3.4.3 Connectome Fingerprinting Performance

The main idea of connectome fingerprinting is to differentiate between individual human based on the connectome profile (Finn et al., 2015). As we explored from the previous performance indicators, it is important for the AI based methods to evaluate the predicted result in a more appropriate way. The traditional fingerprinting is a good way to approximate but as discussed before, there lies some major limitations. By comparing against other functional connectomes, we have developed an accuracy parameter named as Pairwise Functional Connectome Fingerprinting (PFCF). The principle involved with the PFCF is similar as the conventional functional connectome fingerprinting (Finn et al., 2015). However, rather than determining whether each predicted FC could select correctly from the entire pool of measured FCs, the problem was made computationally easier for the algorithm to correctly calculate the overall accuracy. PFCF makes the whole connectome fingerprinting as a series of pairwise tests for each predicted vs. measured FC and keeps track of the number of successful classifications. These procedures are repeated for all participants for calculating an overall

accuracy parameter. For evaluation of the classification, we have used correlation coefficients, and mean squared error. A set of accuracy counters was logically triggered active was based on the comparison with the higher the correlation coefficients and lower the mean squared error. After the comparison was over, the counter was used to calculate the overall accuracy of the algorithm performance. One of the key factors to consider during the fingerprinting process is the usage of both positive and negative connectomes rather than using only the positive connectomes. The connectome domain itself have positive and negative correlations and it would be unwise to consider only the positive connectome for consideration. We have experimented with the idea and found out that it scores perfectly, but this is not the ideal case scenario and thus we wanted to evaluate both the positive and the negative connectome.

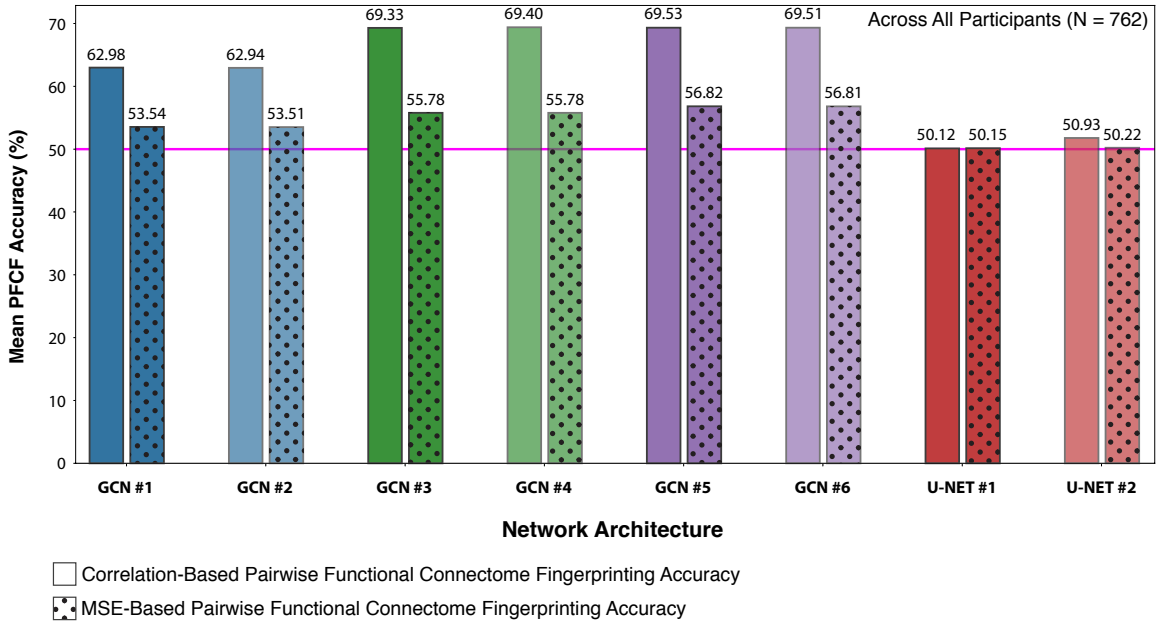

Figure 3.5: Performance evaluation via the PFCF from two different calculation based methods (such as correlation based and MSE based). The higher the accuracy, the higher the chance of finding out the exact connectome based on the chance. The violet line specifies about the mean performance of the algorithm.

As we observe from the Figure 3.5, we have achieved a fingerprinting accuracy of almost 70% for GCN#3 - GCN#6 across all the participants. For all participants, among N_{Trials}= 762 (the number of participant) × 761 (the number of comparison between one to other participants) = 579,882 trails, getting an PFCF just by random

chance is very small as suggested by the binomial probability graph of Figure 2.7 B. From the Figure 3.5, the pink line specifies the Participants Greater Than Chance (PGTC) accuracy which is statistically significant if we only considered the accuracy greater than 50% for all the people. In our case, all our GCNs performance was statistically very significant. Specially, when we added more layers to it (GCN#3 – GCN#6) the mean fingerprinting accuracy increased, suggesting that adding more complexities allowed the GCN-based predictions to become more accurate. In the case of U-Net, the performance is around 50% suggesting that it became almost a chance to find out the correct connectome for a specific participant.

3.5 Discussion

This paper presents an improved algorithm for the prediction of brain functional connectivity from structural connectivity through deep learning architecture. Using a set of performance evaluation parameters that we have evaluated, we can conclude that GCN-based structures are generally more successful in reproducing functional connectivity than U-Net-based architectures. We have experimented with different structural variation of two architectures and evaluated different configuration among them. Using a permutation 3-layer configuration, we were able to get a PFCF of around 70% accuracy in GCN. But in our case, we have experimented with more than three layers (five-layer, seven layer) with GCN but it did not improve the overall performance. Although, theoretically it's not overfitting (as the loss curve is still decreasing but in a small scale), but these added trainable components are making the algorithm hard to optimize. Even adding some other adaptation optimizer like AdaGrad (Lydia & Francis, 2019), RMSProp (Tieleman, Hinton, et al., 2012) was experimented but it did not significantly converge the algorithms train error. In some cases, the performance parameters seem to hit a plateau after different changes in layer configurations. For the case of U-Net, we experimented with shorter and longer convolution and up convolution block, but it did not improve the performance parameters. We assume that it might be a case of degradation problem since neural network are notoriously bad

for finding a simple mapping parameter. That is why we experimented with U-Net with skip connection with the existing architecture to explore how it performed in the prediction problem. In all cases, GCN# 4 - GCN#6 performed better than the other architectural combination. It is only natural to experiment with different architecture with a variation of layer configuration for different types of connectivity analysis. Hopefully this study will pave the way for future AI based brain connectivity analysis.

References

Finn, E. S., Shen, X., Scheinost, D., Rosenberg, M. D., Huang, J., Chun, M. M., Papademetris, X., & Constable, R. T. (2015). Functional connectome fingerprinting: Identifying individuals using patterns of brain connectivity. *Nature neuroscience*, *18*(11), 1664–1671.

Glasser, M. F., Coalson, T. S., Robinson, E. C., Hacker, C. D., Harwell, J., Yacoub, E., Ugurbil, K., Andersson, J., Beckmann, C. F., Jenkinson, M., et al. (2016). A multi-modal parcellation of human cerebral cortex. *Nature*, *536*(7615), 171–178.

Greicius, M. D., Supekar, K., Menon, V., & Dougherty, R. F. (2009). Resting-state functional connectivity reflects structural connectivity in the default mode network. *Cerebral cortex*, *19*(1), 72–78.

Gui, X., Chuansheng, C., Zhong-Lin, L., & Qi, D. (2010). Brain imaging techniques and their applications in decision-making research. *Xin li xue bao. Acta psychologica Sinica*, *42*(1), 120.

He, K., Zhang, X., Ren, S., & Sun, J. (2016). Deep residual learning for image recognition. *Proceedings of the IEEE conference on computer vision and pattern recognition*, 770–778.

Honey, C. J., Kötter, R., Breakspear, M., & Sporns, O. (2007). Network structure of cerebral cortex shapes functional connectivity on multiple time scales. *Proceedings of the National Academy of Sciences*, *104*(24), 10240–10245.

Honey, C. J., Sporns, O., Cammoun, L., Gigandet, X., Thiran, J.-P., Meuli, R., & Hagmann, P. (2009). Predicting human resting-state functional connectivity from structural connectivity. *Proceedings of the National Academy of Sciences*, *106*(6), 2035–2040.

Kim, M., Bao, J., Liu, K., Park, B.-y., Park, H., & Shen, L. (2020). Structural connectivity enriched functional brain network using simplex regression with graphnet. *International Workshop on Machine Learning in Medical Imaging*, 292–302.

Kingma, D., & Ba, J. (2015). Adam: A method for stochastic optimization3rd international conference on learning representations, iclr 2015. *International Conference on Learning Representations, ICLR*.

Kipf, T. N., & Welling, M. (2016). Semi-supervised classification with graph convolutional networks. *arXiv preprint arXiv:1609.02907*.

Li, H., Xu, Z., Taylor, G., Studer, C., & Goldstein, T. (2018). Visualizing the loss landscape of neural nets. *Advances in neural information processing systems*, *31*.

Li, Y., Shafipour, R., Mateos, G., & Zhang, Z. (2019). Mapping brain structural connectivities to functional networks via graph encoder-decoder with interpretable latent embeddings. *2019 IEEE Global Conference on Signal and Information Processing (GlobalSIP)*, 1–5.

Lin, Y., Ma, J., Huang, B., Zhang, J., Zhang, Y., & Dai, Z. (2021). Predicting human intrinsic functional connectivity from structural connectivity: An artificial neural network approach. *IEEE Transactions on Network Science and Engineering*, *8*(3), 2625–2638.

Lydia, A., & Francis, S. (2019). Adagrad—an optimizer for stochastic gradient descent. *Int. J. Inf. Comput. Sci*, *6*(5), 566–568.

Mišić, B., Betzel, R. F., De Reus, M. A., Van Den Heuvel, M. P., Berman, M. G., McIntosh, A. R., & Sporns, O. (2016). Network-level structure-function relationships in human neocortex. *Cerebral Cortex*, *26*(7), 3285–3296.

Paszke, A., Gross, S., Massa, F., Lerer, A., Bradbury, J., Chanan, G., Killeen, T., Lin, Z., Gimelshein, N., Antiga, L., Desmaison, A., Kopf, A., Yang, E., DeVito, Z., Raison, M., Tejani, A., Chilamkurthy, S., Steiner, B., Fang, L., ... Chintala, S. (2019). Pytorch: An imperative style, high-performance deep learning library. In H. Wallach, H. Larochelle, A. Beygelzimer, F. d'Alché-Buc, E. Fox, & R. Garnett (Eds.), *Advances in neural information processing systems 32* (pp. 8024–8035). Curran Associates, Inc. http://papers.neurips.cc/paper/9015-pytorch-an-imperative-style-high-performance-deep-learning-library.pdf

Ronneberger, O., Fischer, P., & Brox, T. (2015). U-net: Convolutional networks for biomedical image segmentation. *International Conference on Medical image computing and computer-assisted intervention*, 234–241.

Smith, S. M., Beckmann, C. F., Andersson, J., Auerbach, E. J., Bijsterbosch, J., Douaud, G., Duff, E., Feinberg, D. A., Griffanti, L., Harms, M. P., et al. (2013). Resting-state fmri in the human connectome project. *Neuroimage*, *80*, 144–168.

Sporns, O. (2007). Brain connectivity. *Scholarpedia*, *2*(10), 4695.

Tieleman, T., Hinton, G. et al. (2012). Lecture 6.5-rmsprop: Divide the gradient by a running average of its recent magnitude. *COURSERA: Neural networks for machine learning*, *4*(2), 26–31.

Van Essen, D. C., Smith, S. M., Barch, D. M., Behrens, T. E., Yacoub, E., Ugurbil, K., Consortium, W.-M. H., et al. (2013). The wu-minn human connectome project: An overview. *Neuroimage*, *80*, 62–79.

Zhang, L., Wang, L., & Zhu, D. (2020). Recovering brain structural connectivity from functional connectivity via multi-gcn based generative adversarial network. *International Conference on Medical Image Computing and Computer-Assisted Intervention*, 53–61.

Chapter 4

General Discussion and Future Directions

4.1 Discussion

In summary, this thesis focused on proposing and optimizing methods for AI-based brain connectivity analysis – specifically the prediction of individual human brain FC connectomes from SC connectomes.

In chapter 2 , we laid the groundwork for subject specific SC to FC prediction by introducing a standardized dataset (along with the atlas for the ROI's) and proposed a set of evaluation metrics along with a novel parameter. As researchers in the brain connectivity domain have worked with different datasets along with different parcellation techniques, it is necessary to provide a standard protocol for future comparisons between different methods of analysis. We also provided a detailed background about the limitations of brain connectivity-based analysis through machine learning methods and proposed an idea for how to evaluate the performance of different algorithms. The fundamental idea is to provide a set of well-established matrices that are currently used for evaluating SC-FC based analysis, to introduce a novel Pairwise Functional Connectome Fingerprinting (PFCF) approach and then demonstrate a proof-of-concept using the standardized, publicly-available dataset. Our experiment showed that PFCF along with other performance parameters can effectively evaluate the performance of the algorithm for subject specific SC-FC prediction. From the earlier testing, it proves to be an effective parameter for evaluating connectome-based analysis for AI-based methods.

In chapter 3, we then built upon our earlier proof-of-concept and compared different implementations of both Graph Convolutional Network (GCN) and U-Net architectures to predict/construct functional connectivity from structural connectivity using a purely data driven processes. Along with all the permutations and combinations of architecture that we experimented, GCN performed better than U-Net in every case. In this chapter, we tried to further explore the idea of PFCF to see how it performed along with the variation of the architectural combination. We started with a baseline GCN and then sequentially introduced different non-linearity for better predicting the functional connectivity. From our initial baseline study, we hypothesized that adding extra layers would give the network leverage to learn new mapping features, thus improving the predicted results. We explored with six different combinations of the GCN architectures and evaluate the performance based on the proposed performance pipeline. Since our task can be easily reconfigured as a matrix-to-matrix reconstruction, we experimented with the U-Net based architecture, where the input to the matrix is structural connectivity and the output to the matrix is predicted functional connectivity. And based on the initial performance, we also experimented with the architectural variation of U-Net using skip connections. The performance parameters discussed in chapter 2 were also implied in the judgement of these configurations of algorithms. From the observation of these performance parameters, we are hopeful that it would pave the way for future exploration for in the SC-FC mapping.

There are several main challenges for the exploration of subject specific SC-FC prediction. Most of the group averaged SC-FC prediction studies considered small atlas like the 68 ROI Desikan-Killiany atlas (Desikan et al., 2006) depending on the availability of dataset that the authors chose. From a data driven process, it is hard to comprehend how those analysis would result if we considered more high-resolution brain parcellations like the 360 ROI Glasser atlas (Glasser et al., 2016). Another challenges were to find out effective mapping from subject specific SC-FC prediction. Despite having correlation between group averaged SC and FC, the specificity of this relationship was not unique to any individual connectomes (Zimmermann et al., 2018).

As the earlier studies experimented with SC-FC mapping, the output is often more of a "generalized version" of the connectivity rather than unique connectivity that any subject contains. Even if we introduce a greater number of layers in the neural network, the performance seems to hit a plateau. Due to the complex mapping between the regions, it becomes hard for the algorithm to learn the unique mapping rather than the general mapping. Due to recent advancement in the applied AI and deep learning structures, we hope that studies will revolve around curated algorithm for SC-FC mapping. And due to the nature of the deep learning-based structures, its interpretability is always a question. In that case we need an algorithm evaluation pipeline to judge the accuracy of the algorithm and through the earlier studies, PFCF can give us the appropriate solution. I believe the thesis has succeeded in achieving the objectives as outlined in Chapter 1 and I also hope that future directions will lead this study into further explorations in brain connectivity domain.

4.2 Future Directions

Although our work represents a very early application of deep learning methods to study human brain connectivity, we anticipate that there will be dramatically increased interest in this emerging field in the coming years. We hope that by helping to lay the groundwork with a standardized dataset, curated set of benchmarking methods, and ultimately providing a proof-of-concept and initial benchmark, that we will have made it easier for other groups (including researchers from different fields), to approach this problem and bring novel solutions that could ultimately help to unravel the mysteries about SC-FC-relationships and how the brain is organized. Since this is so novel, there are so many potential avenues to explore, and deep learning methods are evolving and improving so rapidly, it will be exciting to see where things will be in a decade. However, some obvious avenues for future exploration, include:

4.2.1 Exploring Different Deep Learning Methods and More Architectural Variations

For the future direction, we can always navigate towards different architectural variation of the network. Some recent studies (involving adversarial learning (Zhang et al., 2020), Graph-constrained Elastic Net (Kim et al., 2020), and Graph Neural Net (Neudorf et al., 2022) have demonstrated promising results in the connectivity prediction. Also, experimentation with customized loss function (such as GDL based loss) could navigate towards more appropriate hyperparameter tuning. There are also some unique concepts with the hybridization of different network structures (Singh & Jaiswal, 2021); where two or more network architectures can specifically look for different properties in the output and predict the connectivity. We hope these new trends will discover new parameters towards brain connectivity prediction.

4.2.2 ROI Based Observation for FC or SC Mapping

Earlier studies investigated the mapping of SC or FC based on the whole set of ROI's. From the connectivity map, its observable that not all connectomes contributed equally for the analysis. Rather than looking to the overall atlas, future studies can navigate towards specific connectomes related with specific parts of the brain, such as primary visual cortex or occipital sulcus area. These specific region-based SC-FC connectivity analysis can help the researchers to understand the how individual regions are linked together. It can also navigate towards overall performance improvement towards existing algorithms; such as using any statistical parameters, we can identify which of the regions are predicted better than other regions and accumulate the network based on these configuration.

4.2.3 Exploring Relationships Between SC and Dynamic Functional Connectivity (dFC)

The preprocessed different dynamic functional connectivity matrices could have a separate distinction based on the connectivity prediction. So far, we have analyzed different dynamic connectivity based on the sliding window, but these parameters could be the

key to the future of dynamic connectivity analysis. So far, we have extracted three different dynamic functional connectivity i.e. for capturing higher frequency temporal information. Based on the sliding window mechanisms and the variation of the statistical parameters we can extract different dynamic functional connectivity matrixes. Each of the different dynamic connectivity i.e. that we have derived (dfc_max, dfc_min and dfc_var) have their own unique aspects in individual connectome prediction. For example, dfc_max is extracted using the maximum correlations between the bi-variate correlations. So, the individual subject's SC to dfc_max prediction can direct us towards furthering our understanding about how SC and dFC are linked. Or given a dynamic connectivity (maximum, minimum or variance), can it predict another form of connectivity (or vise-versa). This direction of research towards dynamic connectivity-based brain structure to function mapping can open a new avenue towards connectivity analysis.

4.2.4 Exploring SC-FC Relationships As a Function of Brain Development, Aging, Injury, and Disease

So far, the population of study in SC-FC is geared towards healthy control data of young adults. But there are different avenues we can take for connectivity analysis if we have the necessary datasets based on the age group, such as specific datasets for children or elderly populations. Also, most of the studies are focusing only on the healthy control data. So, there is a certain demand for brain disorders-based connectivity analysis (such as Alzheimer's Disease Neuroimaging Initiative (ADNI) or Parkinson's Disease Progressive Neuroimaging Initiative (PDPNI) (Zhu et al., 2021)) could direct us towards brain connectivity-based analysis on brain disorders. In the future directions of the brain disorder based studies, if the performance were to become good enough, researchers could perhaps even induce artificial SC lesions to simulate focal brain injury or degeneration and gauge how that might effect whole-brain FC. This could be an interesting avenue for novel hypothesis generation, which could then be tested in experimental models. The AI-based analysis is still on its early stages, but new and improved architecture can pave the way for future improvement.

References

Desikan, R. S., Ségonne, F., Fischl, B., Quinn, B. T., Dickerson, B. C., Blacker, D., Buckner, R. L., Dale, A. M., Maguire, R. P., Hyman, B. T., et al. (2006). An automated labeling system for subdividing the human cerebral cortex on mri scans into gyral based regions of interest. *Neuroimage*, *31*(3), 968–980.

Glasser, M. F., Coalson, T. S., Robinson, E. C., Hacker, C. D., Harwell, J., Yacoub, E., Ugurbil, K., Andersson, J., Beckmann, C. F., Jenkinson, M., et al. (2016). A multi-modal parcellation of human cerebral cortex. *Nature*, *536*(7615), 171–178.

Kim, M., Bao, J., Liu, K., Park, B.-y., Park, H., & Shen, L. (2020). Structural connectivity enriched functional brain network using simplex regression with graphnet. *International Workshop on Machine Learning in Medical Imaging*, 292–302.

Neudorf, J., Kress, S., & Borowsky, R. (2022). Structure can predict function in the human brain: A graph neural network deep learning model of functional connectivity and centrality based on structural connectivity. *Brain Structure and Function*, *227*(1), 331–343.

Singh, B., & Jaiswal, R. (2021). Impact of hybridization of deep learning models for temporal data learning. *2021 IEEE 8th Uttar Pradesh Section International Conference on Electrical, Electronics and Computer Engineering (UPCON)*, 1–6.

Zhang, L., Wang, L., & Zhu, D. (2020). Recovering brain structural connectivity from functional connectivity via multi-gcn based generative adversarial network. *International Conference on Medical Image Computing and Computer-Assisted Intervention*, 53–61.

Zhu, S., Ju, Z., Wu, P., Liu, F., Ge, J., Zhang, H., Lu, J., Li, L., Wang, M., Jiang, J., et al. (2021). The parkinson's disease progression neuroimaging initiative. *Behavioural Neurology*, *2021*.

Zimmermann, J., Griffiths, J., Schirner, M., Ritter, P., & McIntosh, A. R. (2018). Subject specificity of the correlation between large-scale structural and functional connectivity. *Network Neuroscience*, *3*(1), 90–106.